# *Quantifying renewable energy potential and realised capacity in India: opportunities and challenges*

Received: 2 May 2023 | Revised: 30 January 2024 | Accepted: 11 March 2024

DOI: 10.1002/met.2196

RESEARCH ARTICLE

Meteorological Applications
Science and Technology for Weather and Climate
Open Access
RMetS

# Quantifying renewable energy potential and realized capacity in India: Opportunities and challenges

**Kieran M. R. Hunt**[1,2] | **Hannah C. Bloomfield**[3,4]

[1]Department of Meteorology, University of Reading, Reading, UK

[2]National Centre for Atmospheric Sciences, University of Reading, Reading, UK

[3]Department of Geographical Sciences, University of Bristol, Bristol, UK

[4]Department of Civil and Geospatial Engineering, School of Engineering Newcastle University, Newcastle upon Tyne, UK

**Correspondence**
Kieran M. R. Hunt, Department of Meteorology, University of Reading, Reading, UK.
Email: k.m.r.hunt@reading.ac.uk

**Funding information**
Natural Environment Research Council, Grant/Award Numbers: NE/V017756/1, NE/W007924/1

**Abstract**

As both the population and economic output of India continue to grow, so does its demand for electricity. Coupled with an increasing determination to transition to net zero, India has responded to this rising demand by rapidly expanding its installed renewable capacity: an increase of 60% in the last 5 years has been driven largely by a quintupling of installed solar capacity. In this study, we use broad variety of data sources to quantify potential and realized capacity over India from 1979 to 2022. For potential capacity, we identify spatiotemporal patterns in solar, wind, hydro and wave power. We show that solar capacity factor is relatively homogeneous across India, except over the western Himalaya, and is highest during the pre-monsoon. Wind capacity factor is highest during the summer monsoon, and has high values off the southern coast, along the Western Ghats, and in Gujarat. We argue that wave power could be a useful source of renewable energy for the Andaman and Nicobar Islands, which are not connected to the main Indian power grid. Using gridded estimates of existing installed capacity combined with our historical capacity factor dataset, we create a simple but effective renewable production model. We use this model to identify weaknesses in the existing grid—particularly a lack of complementarity between wind and solar production in north India, and vulnerability to high-deficit generation in the winter. We discuss potential avenues for future renewable investment to counter existing seasonality problems, principally offshore wind and high-altitude solar.

**KEYWORDS**

climate, hydro power, India, renewable energy, solar power, wind power

## 1 | INTRODUCTION

### 1.1 | Renewable energy in India

Global increases in renewable energy are required to meet carbon mitigation targets. India is increasingly investing in renewables (including wind, solar and hydro). As of July 2023, India has 179 GW of renewables installed including 42.8 GW of wind power, 67.1 GW of solar power and 46.9 GW of large hydropower (Indian Power Industry, 2023). The potential for further renewables to be built over India is very high for wind power

(Deshmukh et al., 2017, 2019; Hossain et al., 2016), solar power (Deshmukh et al., 2017, 2019; Jain et al., 2020; Mahtta et al., 2014; Muneer et al., 2005), and hydropower (Xu et al., 2023). Currently, all of India's wind power generation is onshore. There are downsides to onshore wind, including land acquisition issues, turbine noise disruption and potential disruption to bird migration patterns (Saidur et al., 2011). Therefore, offshore wind potential off the coast of India is also being investigated (Hossain et al., 2016; Kulkarni et al., 2018a), although some of these factors could still be an issue. New developments in floating wind farms, which reduce the usual depth requirements of ~50 m for fixed foundation wind farms to much larger values, increase the viability of offshore wind for India (Wu et al., 2019).

Power system modelling simulations show that it is possible for India to meet its climate mitigation targets by adopting large shares of renewable generation if it is complemented by large-scale installation of storage technologies to meet demands in times of particularly low renewable generation output (Gulagi et al., 2017, 2020; Lu et al., 2020; Lugovoy et al., 2021). One of the key challenges for operating resilient power grids with large penetrations of renewables is managing the variability of weather-dependent renewables (Bloomfield et al., 2016). Both synoptic conditions and local disturbances can influence renewable generation outputs (as outlined in Section 1.3). Managing this variability is an ongoing challenge for transmission and distribution grid operators.

## 1.2 | Managing renewable variability

Historically, grid resilience would have been managed using metered demand and supply time series. However, with the increasing quantities of renewable generation now being installed and the rapid electrification of the heat and transport sectors, historical data are now a poor proxy to understand real-time grid operations (Bloomfield et al., 2021). Reanalyses have therefore become a key meteorological data source to quantify renewable variability in regions where metered data sources are sparse. These gridded optimal combinations of meteorological observations and a numerical weather prediction model can be used to produce synthetic demand and renewable time series for historical periods to characterize variability (e.g., Bloomfield, Brayshaw, et al., 2022; Dubus et al., 2022; Pfenninger & Staffell, 2016; Staffell & Pfenninger, 2016), which then become inputs for power system modelling simulations. These synthetic renewable datasets are generally validated on historical observations (e.g., from the ENTSO-e Transparency Platform for Europe, https://transparency.entsoe.eu/). However, such observations are not always available for developing regions in an easily accessible format (or the renewable generation may not be built yet), so theoretical generation profiles are often calculated instead (Bloomfield, Wainwright, et al., 2022; Dunning et al., 2015).

Previous reanalysis-based work over India has focused on the seasonal balance of demand and wind power generation, particularly focusing on the impact of the Indian monsoon. Dunning et al. (2015) showed that during active monsoon phases there tends to be lower temperatures (suggesting a reduced requirement for air conditioning demand) and strong winds, therefore high wind power output; whereas monsoon breaks tend to be associated with higher temperatures (so increased demand) and reduced wind power generation. The break phases also are associated with dry spells, so increased agricultural demand for water pumping (Kulkarni et al., 2018b). Alongside this, Gopi et al. (2021) showed that PV plants in southern India experience reduced output during the monsoon period due to increased cloud cover. The spatiotemporal complementarity of wind and solar has been highlighted as a potential way to 'overcome the monsoon hurdle' (Gulagi et al., 2020).

On shorter timescales, a particular resilience challenge to highly renewable systems are multi-day periods of low renewable generation, often termed wind droughts, or *dunkelflaute* if solar generation is also included. Gangopadhyay et al. (2022) investigated the potential for these periods of prolonged low wind generation over India using a stochastic weather generator, finding that there tend to be dipoles in generation availability between Rajasthan (northwest India) and southern India. This suggests that regional-scale wind droughts could be avoided through good interconnection of neighbouring energy grids.

## 1.3 | The weather and climate of India

India has a diverse range of climate zones, including tropical lowlands and coastal hills in the south, arid regions in the west, mountains across the north and temperate zones in the northeast (Beck et al., 2018). Straddling both the tropics and subtropics, India undergoes complex annual variations in weather, which could impact renewable power production. This can broadly be categorized into four seasons.

Perhaps the most prominent of these is the summer monsoon, whose onset slowly covers the country from south to north throughout June, and which then slowly withdraws in the opposite direction during September (Fasullo & Webster, 2003). The summer monsoon is at full strength in July and August, although it is impacted by significant

intraseasonal variability. The majority of mean and extreme precipitation in the summer monsoon, as well as its strongest winds, are associated with the passage of monsoon low-pressure systems (LPSs; Hunt & Fletcher, 2019; Thomas et al., 2021). The monsoon is fed by moisture brought to the subcontinent by the Somali jet, which provides constant, reasonably strong, low-level westerlies to the south and centre of the peninsula. The resulting widespread precipitation is also associated with heavy cloud cover.

Following the withdrawal of the summer monsoon, the subcontinent experiences post-monsoon conditions, which persist through October and November until the arrival of the upper-level subtropical jet over northern India, which marks the start of winter. North Indian Ocean tropical cyclones are most common during this season (Mohapatra et al., 2012). The other important feature of this season is the so-called 'northeast monsoon', where northeasterly winds bring heavy precipitation to southeast India (Dhar & Rakhecha, 1983; Rajeevan et al., 2012).

The subtropical jet starts to move over north India in December and is at its strongest during January and February. It then weakens and withdraws northward throughout March and April (Schiemann et al., 2009). The presence of the subtropical jet marks the winter season, which is characterized by dry conditions across southern India, while winter storms—known as western disturbances—impact north India, particularly along the Himalayas, bringing large-scale cloud cover and precipitation (Dimri et al., 2015; Hunt, Turner, & Shaffrey, 2018).

The period after the withdrawal of the subtropical jet but before the onset of the summer monsoon is marked by long spells of clear, dry conditions and weak winds, particularly in north and central India. This is typically referred to as the pre-monsoon and reaches its height in April and May. The majority of heatwaves in India occur during these months, and so the demand for air conditioning is at its highest (Ratnam et al., 2016).

### 1.4 | Research outline

This study extends the analysis from the previously discussed papers to present the first fully open access reanalysis-based reconstruction of existing renewable generation in India (code available at https://github.com/kieranmrhunt/india-renewable and data available at https://doi.org/10.5281/zenodo.7824872). Using this state-of-the-art dataset, we:

- explore the theoretical potential of renewable generation across India and propose optimal regions for future developments;
- present open access newly validated models of regional wind and solar PV generation over India, based on locations of existing renewable plants;
- quantify the spatiotemporal complementarity between wind and solar power across India;
- highlight key time periods where the present-day power system may be exposed to resilience challenges; and
- explore the impact of future wind and solar PV generation on grid robustness.

This article is organized as follows. Section 2 outlines the datasets used in the study (including hydrometeorological and energy-sector data). Following this, methods to create renewable capacity factors are described (Section 2.3) and applied to the existing Indian renewable energy fleet (Section 2.4) followed by some model verification (Section 2.5). The results start by outlining the theoretical capacity of the renewable generation (Section 3). In the remainder of the article, the focus is on some useful applications including the wind–solar complementarity (Section 4.1), extreme generation times (Section 4.2) and mechanisms to improve grid robustness (Section 4.3). The article concludes with a discussion of key findings and avenues for future work (Section 5).

## 2 | DATA AND METHODS

### 2.1 | Hydrometeorological data

#### 2.1.1 | ERA5

ERA5 is the fifth generation atmospheric reanalysis of global climate produced by the Copernicus Climate Change Service at the European Centre for Medium-Range Weather Forecasts (Hersbach et al., 2020). Data from ERA5 (available from https://cds.climate.copernicus.eu/cdsapp#!/home) cover the entire globe at a horizontal resolution of ∼25 km and resolve the atmosphere on 137 levels from the ground up to 80 km in altitude. It covers from January 1940 until present at hourly frequency. We use single-level data (https://doi.org/10.24381/cds.adbb2d47) to investigate fields closely related to renewable power generation: 100-m winds, 2-m temperature, downward shortwave radiation at the surface and selected ocean wave fields. ERA5 is commonly used as a tool for energy-meteorology analysis due to the limited length of observational records from existing renewable facilities.

#### 2.1.2 | GloFAS

The worldwide Global Flood Awareness System (GloFAS; Harrigan et al., 2020), created collaboratively by the European Commission and the European Centre for Medium-Range Weather Forecasts, is a global hydrological forecasting and monitoring system that is not constrained by administrative or political boundaries. It combines cutting-edge meteorological predictions with a hydrological model, and due to its continental scale set-up, it can deliver information on upstream river conditions as well as continental and global overviews to downstream nations. Hydrological data from GloFAS are freely available from the Copernicus Climate Data Store (https://cds.climate.copernicus.eu/#!/home). In this article, we use GloFAS-ERA5 (Zsoter et al., 2019), a global modelled dataset of daily river discharge created by forcing the hydrological model with the ERA5 reanalysis (https://doi.org/10.24381/cds.a4fdd6b9). This co-occurrence with the ERA5 reanalysis is key when considering the complementarity of existing and potential renewable generation. These data are global, have daily frequency and a resolution of $0.1^\circ \times 0.1^\circ$.

### 2.2 | Renewable installation and generation data

#### 2.2.1 | OpenStreetMap

OpenStreetMap (OpenStreetMap contributors, 2017) (OSM) is a collaborative project to create a free, editable map of the world. It allows users to view, edit and add data, and has a large user community that contributes data on a wide range of topics, including location names, road networks and points of interest. It is a popular choice for many users because it is open and accessible. However, the quality and completeness of the data can vary because it relies on the contributions of volunteers. In this study, we use OSM data for a brief qualitative analysis of the locations of renewable power installations across India. Sample code for extracting location data is given in the Appendix.

#### 2.2.2 | Central electricity authority

We used two sets of Central Electrical Authority (CEA) data in this study. The first is a report, published in March 2020, which is now archived at https://cea.nic.in/old/reports/others/planning/rpm/Plant-wise\%20details\%20of\%20RE\%20Installed\%20Capacity-merged.pdf. This 1958-page PDF document contains information on all solar, wind and small hydro installations across India, merged from individual state reports. Each entry gives the name of the installation owner, the installed capacity, the date of installation and some location information. This ranges in detail from a street address to a district name. To extract these data, which are stored in tables of varying structure and depth, we wrote a Python script using the tabula and geopy libraries, implementing the Nominatim API for Open Street Maps to convert addresses and district names to longitudes and latitudes. We used these data to estimate the geospatial distribution of installed renewable capacity across India. We provide this parsing script in our repository.

We also used summary large hydro data from CEA to complete Table B1. These data are available from https://cea.nic.in/installed-capacity-report/?lang=en.

#### 2.2.3 | The wind power database

Information about existing and planned wind farms are also available from the Wind Power database (available to purchase from thewindpower.net). Amongst many variables, this includes location, total power, hub-heights and details of the installed capacity of turbines. A version of the database used in this study is taken from October 2021. This has 33 GW of wind power generation available over 914 sites across India. This database is systematically verified and updated twice a year at a minimum and is commonly used by the energy-meteorology community. The global coverage of this dataset and need for manual verification of new entries may be why it reports lower values than the approximately 42 GW identified in the CEA datasets (see Table 1).

#### 2.2.4 | Satellite-derived solar installations

The geospatial estimate of installed solar capacity over India comes from Kruitwagen et al. (2021). They implemented an image segmentation algorithm based on a convolutional neural network and applied it to high-resolution satellite imagery to create a global catalogue of photovoltaic (PV) cell locations. They identified 68,661 units globally, with a total generating capacity of $432 \pm 76$ GW. Their dataset is valid as of 30 September 2018, at which point they estimated the installed PV solar capacity over India to be about 31 GW. This includes private and domestic PV installations, which are not necessarily connected to the grid and is thus higher than the CEA estimate for the same date (24 GW; see Figure 1). Data were downloaded from https://zenodo.org/record/5005868.

**TABLE 1** Summary of the data released with this article, available from the dedicated repository: https://doi.org/10.5281/zenodo.7824872.

| Data description | Figure/Table | File name | Dates valid |
|---|---|---|---|
| Installed capacity by type in each state | Table B1 | installed-by-state-oct2022.csv | Oct 2022 |
| All-India installed capacity by type | Figure 1 | tabulated-installed-by-date.csv | 2017–2023 |
| Present-day installation locations | Figure 2 | OSM_[hydropower,wind_turbine,solar]_installations.geojson | Mar 2022 |
| Gridded 1° × 1° estimate of installed wind/solar capacity | Figures 3a and 4a | CEA_1x1_gridded_installed_[wind,solar]_cap.nc | May 2021 |
| Gridded 1° × 1° estimate of installed wind | Figure 3b | TWP_1x1_gridded_installed_wind_cap.nc | May 2021 |
| Gridded 1° × 1° estimate of installed solar | Figure 4b | K21_1x1_gridded_installed_solar_cap.nc | Sep 2018 |
| Reported daily wind/solar/hydro production | Figures 5 and S5 | POSOCO_reported_[wind,solar,hydro]_MU_daily.csv | 2012–2023 |
| Modelled 'historical' production | Figures 5, 10, S6a,b | modelled-historical-[daily,hourly]-renewable_output.nc | 1979–2022 |
| Hourly wind capacity factor | Figure 6 | wind_capacity_factor.zip | 1979–2022 |
| Hourly solar capacity factor | Figure 7 | solar_capacity_factor.zip | 1979–2022 |
| Recommended locations for new wind/solar installations | Figure 11 | areas-for-exploration.nc | - |

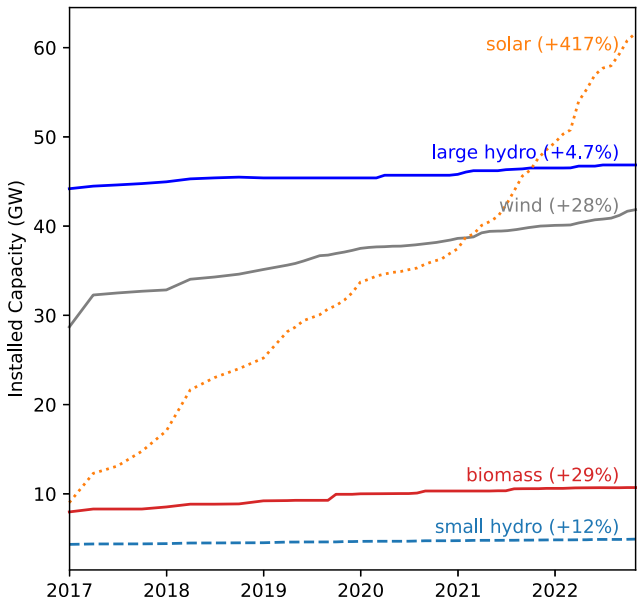


**FIGURE 1** Installed capacity of different types of renewable energy over India. For each type, the values in brackets indicate the growth over the last 5 years (i.e., between October 2017 and October 2022). Large hydro describes installations with nominal power output exceeding 25 MW. Data from the CEA.

### 2.2.5 | Grid-India

Grid-India, formerly known as POSOCO (Power System Operation Corporation Ltd), is a corporation owned by the Indian Ministry of Power, responsible for monitoring supply to and demand from the Indian national energy grid. As part of their remit, they publish monthly reports (https://posoco.in/en/reports/monthly-reports/) on regional energy production by type (for both renewables and non-renewables). We scraped these reports to extract the daily average production for wind, solar and hydro for each of the five regions defined by the grid authorities (north, northeast, south, east and west).

## 2.3 | Capacity factors

### 2.3.1 | Wind turbine capacity factor

Wind power capacity factors are generated using a physical model. To calculate wind power generation, it is necessary to make assumptions about the type of wind turbines installed, as different turbines respond differently at different wind speeds and the 'most suitable' turbine is usually selected as part of the wind farm commissioning process. In this study, hourly gridded 100-m wind speeds from the ERA5 reanalysis (Hersbach et al., 2020) are passed through representative power curves. Here, three representative power curves are considered, representing type 1, 2 and 3 wind turbines in the International Electrotechnical Commission wind speed classification (International Electrotechnical Commission, 2005), as used in Lledó et al. (2019). The details of these are given in the supplement of Bloomfield et al. (2020). In each grid box, the annual mean capacity factors are

assessed over the ERA5 period (1979–2020) and the type of turbine that maximizes the wind power production is chosen to represent that grid square. Figure S1 shows that the type 2 wind turbine was most appropriate for representing wind generation over most of India. However, further offshore, type 1 wind turbines become more prevalent due to the increased average wind speeds.

The power curves represent the relationship between hub-height wind speed and capacity factor (CF), which is calculated as

$$\mathrm{CF}(U_{100},t)=\frac{\mathrm{Generation}(U_{100},t)}{\mathrm{Max.\ Generation}(U_{100},t)}, \quad (1)$$

where $U_{100}$ is the gridded 100-m wind speed and $t$ is time. Generation is the hourly output of a wind turbine (in MW) and Max. generation is the rated output of a turbine (in MW). CF values range between 0 and 1. The gridded wind power CF can then be weighted by the installed capacity in each grid box as a fraction of the national total and aggregated to give a country-aggregate or regions CF time series. This method performs well over Europe with an average $R^2$ of 0.92 and RMSE of 10% (Bloomfield et al., 2020). See Section 2.5 for Indian verification.

### 2.3.2 | Solar panel capacity factor

To estimate solar capacity factor, we follow Bloomfield et al. (2020), using a solar PV model based on the empirical formulation of Evans and Florschuetz (1977), but adapted to reflect newer solar PV technologies using methods from Bett and Thornton (2016). The meteorological inputs are grid-point 2-m-temperature and incoming surface solar shortwave irradiance ($G$), from which gridded solar power capacity factor is calculated as

$$\mathrm{CF}(G,T,t)=\eta(T(t))\frac{G(t)}{G_{\mathrm{ref}}}, \quad (2)$$

where $G(t)$ is the incoming (i.e., downward) shortwave radiation at the surface, $G_{\mathrm{ref}}=1000\ \mathrm{W\,m^{-2}}$, $T(t)$ is the environmental 2-m temperature (with which the PV cell is assumed to be in equilibrium) and $\eta$ is the relative efficiency, given by

$$\eta(t)=\eta_{\mathrm{ref}}(1-\beta_{\mathrm{ref}}(T(t)-T_{\mathrm{ref}})), \quad (3)$$

where $\eta_{\mathrm{ref}}=0.9$, $\beta_{\mathrm{ref}}=0.042$ and $T_{\mathrm{ref}}=25^{\circ}\mathrm{C}$. Bloomfield et al. (2020) reported that the model performs well over Europe, with an average daily $R^2$ of 0.93 with 3.2% error for countries where data were available at high enough quality for validation from power grid observations. See Section 2.5 for Indian verification.

## 2.4 | Existing installed renewable capacity

In this section, we aim to provide reliable estimates of the geospatial distributions of the installation densities and capacities of renewable power installations in India. By comparing estimates from different sources acquired using different methods, we can quantify how reliable the estimates are. In the following section, we then use these estimates to build and verify a simple production model.

We start with the OSM dataset, as shown in Figure 2. Aside from the advantages and disadvantages mentioned in Section 2.2.1, one disadvantage of using this dataset is that entries for renewable power installations, such as wind farms and hydroelectric plants, very rarely have capacity information available for India. Regardless, it is still useful to discuss installation density as it is closely related to capacity density and will provide a helpful comparison.

The OSM dataset indicates that wind turbines and wind farms are currently concentrated along the west coast, particularly in the Rann of Kutch (western Gujarat and western Rajasthan) and along the southern part of the Western Ghats. There are very few installations along the east coast, despite the good wind capacity factor in that region (Section 3.1).

Solar power installations are more evenly spread across India, with much of the south having some coverage. This is a result of the increasing affordability of installing solar panels, which has led to many rooftops being fitted with them (see Table B1). Larger concentrations generally reflect low-altitude areas with higher capacity factors, such as southeast and northwest India.

Hydroelectric power plants are scattered across the subcontinent, but the highest concentrations are found along the Himalayas, particularly in Nepal, which depends heavily on hydropower (International Hydropower Association, 2022). There are also many installations along the Western Ghats, which has a particularly high number of older dammed reservoirs (Hunt & Menon, 2019). However, there are very few hydroelectric installations in Arunachal Pradesh, despite its high suitability. In subsequent sections, we have not sought to produce a gridded estimate of installed hydropower capacity because while there are satellite-derived catalogues of dams and reservoirs (e.g., Mulligan et al., 2020;

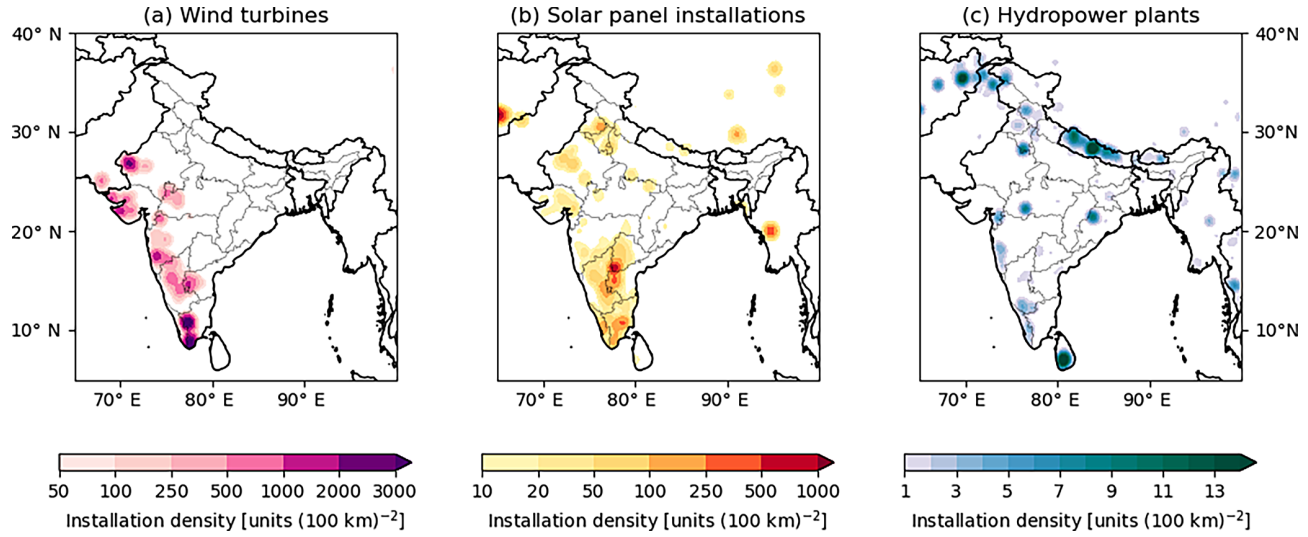


**FIGURE 2** Estimated density (units per 10,000 km$^{-2}$) of installed (a) wind turbines, (b) solar panels and (c) hydropower plants (both large and small) from labelled objects in Open Street Map data.

Wang et al., 2022), there is little information on whether they are used for water storage or power generation, and even less information on what the capacities are. Precise quantification of the capacity density of these installations is therefore left for future work.

### 2.4.1 | Wind

We will now estimate the density of installed wind and solar capacity using information from various sources and quantify the associated uncertainty. The gridded estimates of installed density will allow us to analyse the reliability of the current renewable network and make evidence-based recommendations for improvements later in the article.

The sources for installed wind capacity are the CEA (Section 2.2.2), the Wind Power (TWP) (Section 2.2.3) and the MNRE (Table B1). We resample the point-based data from the CEA and TWP to a $1^\circ \times 1^\circ$ grid. MNRE provides state totals, which we convert to the same units as the gridded data by dividing through by the state areas. The choice of resolution is effectively a compromise between avoiding too coarse a resolution that variability in underlying weather conditions is not well captured and too fine a resolution that small uncertainties in installation locations drive large uncertainties in gridded capacity density. A resolution of $1^\circ$ is appropriate for both wind and solar, whose precursor weather conditions typically vary over spatial scales larger than this (Figures S2 and S3).

The results, shown in Figure 3, indicate that the gridded CEA and TWP data are in close agreement, sharing consensus on the locations of hot spots and dead zones, as well as the overall distribution. As they come from independent sources, their agreement is encouraging, although we note there still could be unreported farms in both. This is confirmed by comparison with the MNRE state totals (Figure 3) and similarity with the OSM installation density (Figure 2a).

Installed wind capacity is mostly concentrated along the western edge of the Indian peninsula, with higher densities along the Western Ghats, along the coast and in the Rann of Kutch. The two largest wind farms in India, the Muppandal Wind Farm in Tamil Nadu on the very southern tip of India and the Jaisalmer Wind Park in far western Rajasthan, respectively the third and sixth largest in the world at present and the only two in India with stated capacity exceeding 1 GW, are visible in both datasets but are more pronounced in the TWP data. There is no installed wind capacity in any of the northern or eastern states. There is also no installed offshore wind capacity and only very sparse installed capacity along the eastern coast, despite both regions having very high capacity factors.

### 2.4.2 | Solar

Estimates of installed solar capacity density (Figure 4) are taken from the same sources as for wind, except we replace data from TWP with data from Kruitwagen et al. (2021) (Section 2.2.4). The two gridded point-source datasets are not in as good agreement as for wind, with the satellite-based dataset estimating a broader overall coverage. However, the two do agree on higher densities on

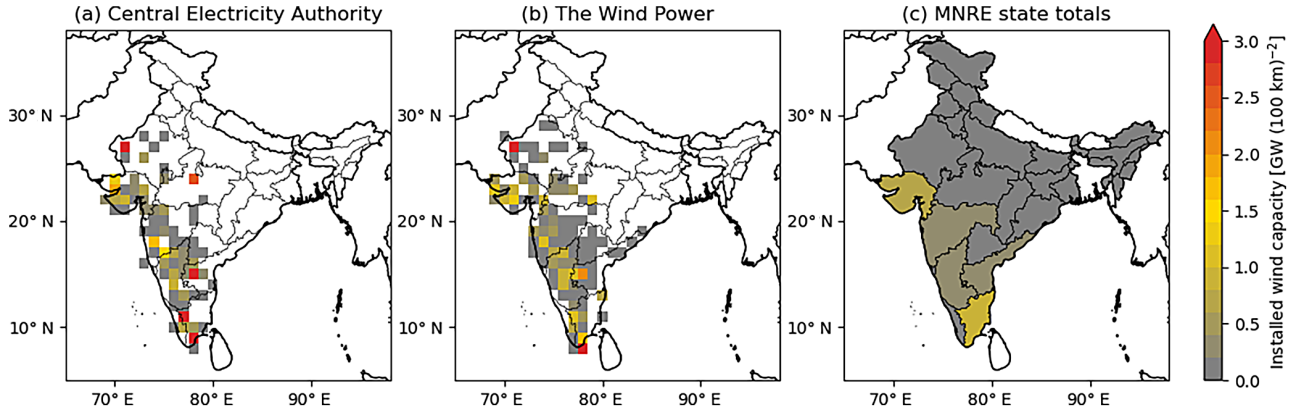


**FIGURE 3** Estimates of installed capacity (GW per 1° gridbox) for wind turbines, using data from (a) the Central Electricity Authority, (b) thewindpower.net and (c) the Ministry of New & Renewable Energy. MNRE data (see Table B1) are provided at the state level and have here been converted to the same density units used in (a) and (b). State boundaries of India are marked.

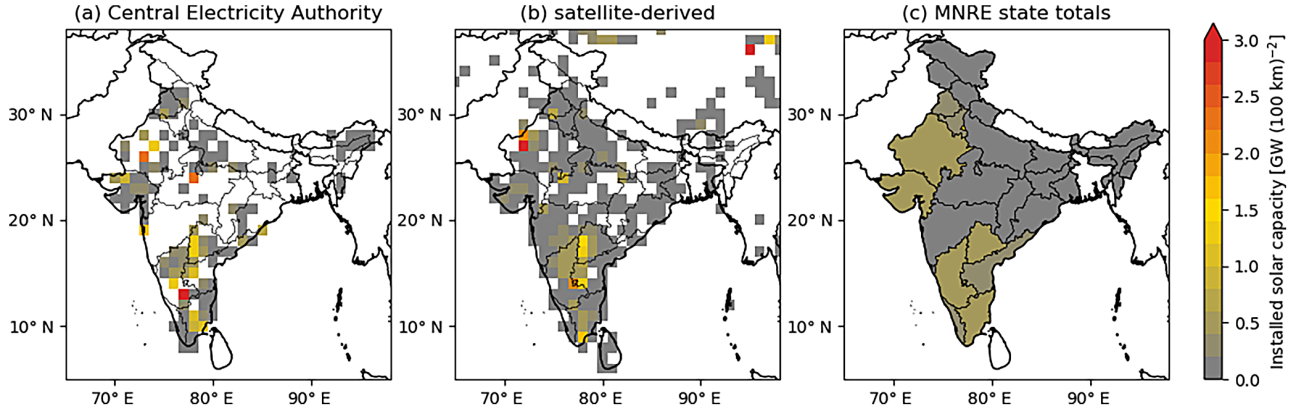


**FIGURE 4** Estimates of installed capacity (GW per 1° gridbox) for solar panels, using data from (a) the Central Electricity Authority, (b) Kruitwagen et al. (2021), and (c) the Ministry of New & Renewable Energy. MNRE data (see Table B1) are provided at state level and have been converted to the same density units used in (a) and (b). State boundaries of India are marked.

the eastern slopes of the Western Ghats and in the north-western states. Comparison with the MNRE state totals and the OSM installation density (Figure 2b) confirms the importance of these two regions and suggests that both gridded datasets have a reasonably high accuracy.

Due to the relative ease of installation, solar production of some magnitude can be found in every Indian state. However, there is almost no installed capacity at higher altitudes (>2000 m), despite the potential advantages in regions such as Ladakh, which remains relatively cloudless during the monsoon. Given the slight divergence between the two gridded estimates of installed capacity for both wind and solar, we used an average of CEA and TWP as our estimate for installed wind capacity and an average of CEA and satellite-derived as our estimate for installed solar capacity. The disagreements are minor, so we have confidence in both estimates, but will test their robustness more rigorously in the next section.

Figure 2 also shows an estimate of hydropower plant density (Figure 2c). These are largely concentrated in orographic regions, particularly the central Himalaya, but are also found along many major rivers. See the Supplementary Material for a more in-depth discussion of hydropower potential in India.

## 2.5 | Renewable production model verification

To confirm the accuracy of both our capacity factor and gridded installation capacity datasets, we combine them to estimate daily renewable power generation over India between January 2020 and October 2022 (Figure 5). Such a model has additional benefits; for example, later in this article, we use it to identify deficit and surplus production days and to identify strategies to reduce production

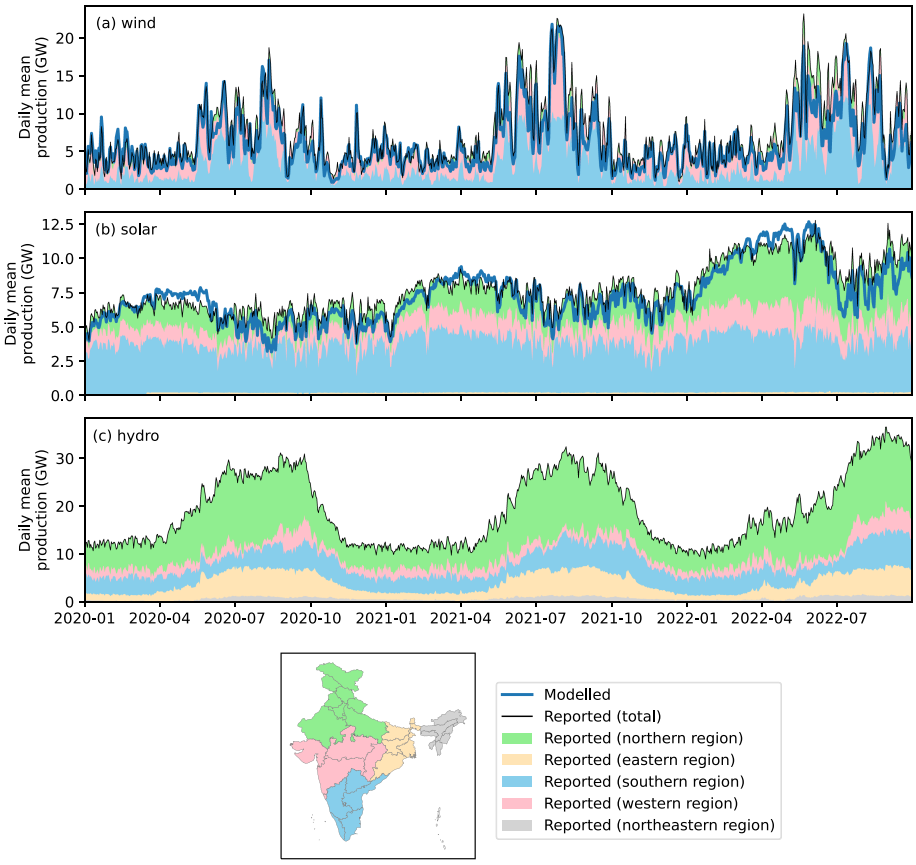


**FIGURE 5** Comparison of reported and modelled renewable power generation in India between January 2020 and October 2022, split into (a) wind, (b) solar and (c) hydropower. We do not model hydropower generation in this study. Reported totals are also broken into contributions from the northern (green), eastern (yellow), southern (blue), western (pink) and northeastern (grey) regions. Reported data have been scraped from Grid-India monthly reports (see Section 2.2.5). The model takes daily mean capacity factors from Section 3, computes a weighted spatial average using the installation data in Section 2.4 and then scales using monthly reported all-India installed capacity (Figure 1).

seasonality. We construct the modelled daily production time series (thick blue lines in Figure 5) by taking the full capacity factor datasets (hourly frequency, $0.25° \times 0.25°$), converting them to daily frequency by taking the diurnal mean, and then compute a normalized weighted average in space using our earlier gridded estimates of installation capacity as the weights. The final step is then to multiply the daily time series of the weighted mean capacity factor by the monthly published installed capacity figures (Figure 1) to account for changes in installed capacity over time.

This relatively simple method provides accurate models whose outputs closely resemble the daily production data provided in Grid-India reports. The linear regression coefficient between the modelled and actual wind production is 0.922. For solar production, it is 0.951. Both models consistently capture short surges and troughs in production. Combined, this gives us confidence to use the model to identify weaknesses and potential improvements in India's renewable grid structure. As mentioned earlier, we do not model hydropower due to lack of installed capacity information (Section 2.4) and due to the large uncertainties introduced by human intervention.

For the interested reader, the full time series of Grid-India daily production data, running from 2012 to 2022, is given in Figure S5.

# 3 | POTENTIAL CAPACITY

## 3.1 | Wind

To assess regions suitable for wind turbines, we compute wind capacity factor for the turbines described in Section 2.3.1. We show the seasonal and spatial patterns in Figure 6.

Wind capacity factor is typically much higher over the surface of the ocean than over land, and is much higher during the summer monsoon than in any other season. Exceptions to the monsoon maximum include the Tibetan Plateau (largest capacity factor in the winter) and a small band along the Himalayan foothills (largest capacity factor during the pre-monsoon). For context, in Europe, regions experiencing annual mean capacity factors above 0.3 are considered the most cost-effective sites for wind power generation (Boretti & Castelletto, 2020).

There are three regions of interest over land where wind capacity factor is markedly higher than elsewhere: the Rann of Kutch, the Tibetan Plateau and the Western Ghats (including northern Sri Lanka). The Western Ghats have particularly high wind speeds during the monsoon as the strong monsoonal westerlies described above are often strong enough to flow over them (Phadtare et al., 2022).

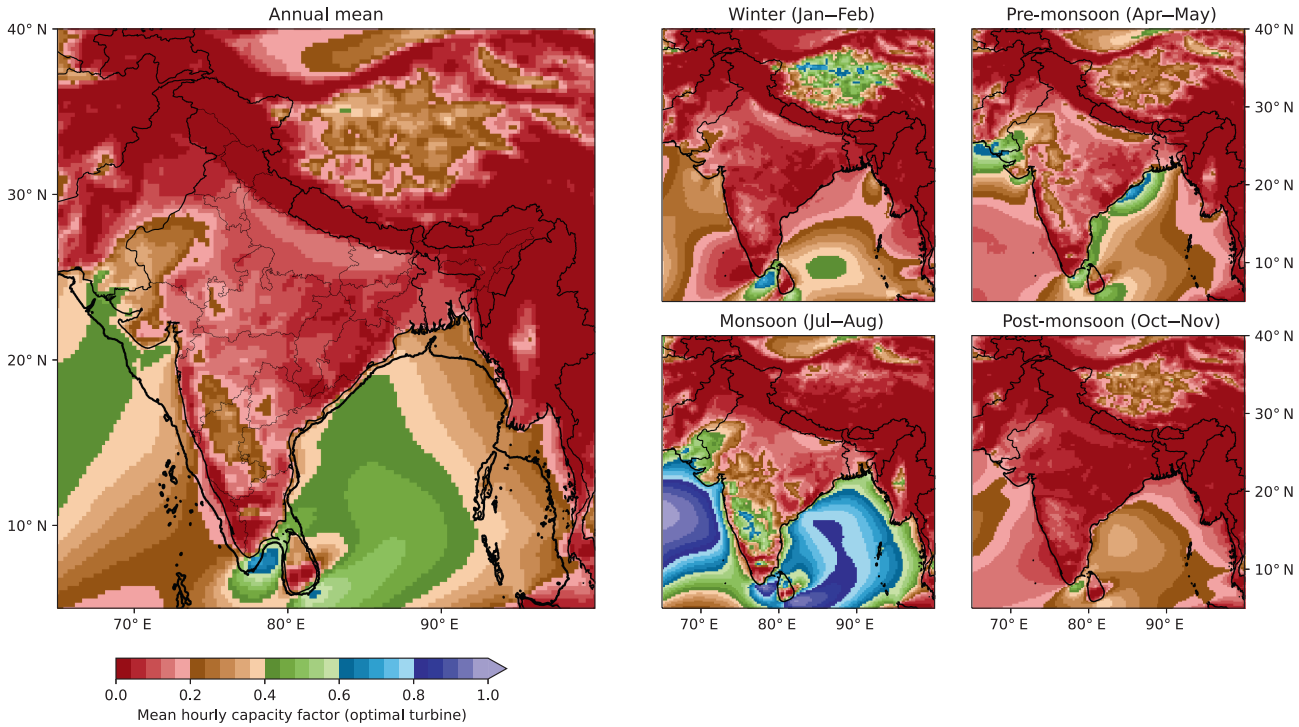


**FIGURE 6** Mean hourly capacity factor for wind over India and the surrounding region from 1979 to 2020. The mean capacity factor is computed for each of the three turbine models described in Section 2.3.1 with the largest of the three (for each grid point) is shown here. The large panel on the left shows the annual mean as well as the state boundaries within India. The four smaller panels on the right show seasonal means of the same field.

The Rann of Kutch (spanning from northern Gujarat to southeastern Pakistan) comprises vast areas of flat salt marshes, meaning that stronger offshore winds can travel relatively undisturbed after making landfall here, particularly when they are orientated perpendicular to the coast, as during the pre-monsoon and monsoon seasons. Like most of the subcontinent, the Rann of Kutch has its highest wind capacity factor during the summer monsoon; however, it maintains a relatively good baseline of generation across the year, and, due to the passage of western disturbances, is almost the only place in India to have a capacity factor larger than 0.2 during the winter months.

While the Western Ghats have some of the highest values of wind capacity factor (exceeding 0.6 during the monsoon), wind energy production here would be highly seasonal, meaning turbines would produce very little energy for two thirds of the year.

Despite its complex orography, the Tibetan Plateau, to the north of India, also records notably high wind power capacity factors. These occur outside of the summer monsoon, when the subtropical jet spends most of its time over the Plateau (Schiemann et al., 2009), supporting mesoscale storms known as Tibetan Plateau vortices (Curio et al., 2019; Hunt, Curio, et al., 2018). Outside of the summer monsoon, the Tibetan Plateau is the biggest potential source of wind energy; however, except for a very small region in east Ladakh, it lies entirely outside of India and would not, therefore, help the Indian grid offset the monsoon maximum. One region that could be considered for this, however, is a band along the base of the central Himalayan foothills, to the south of Nepal, which has a high wind capacity factor during the pre-monsoon. The pre-monsoon is perhaps the most important season for reliable energy generation, as this is when fatal heatwaves predominantly occur (Rao et al., 2021).

It is also worth noting the importance of the climatological angle between wind and mountain ranges. There is almost no wind capacity in the Himalayas and their foothills, where the strongest winds run parallel to the mountain ranges. In contrast, the Western Ghats—where the strongest winds flow perpendicular to the range—have a very high capacity factor.

As is the case globally, wind speeds in the boundary layer are generally much larger over the ocean than over land due to increased friction over the latter. Frictional drag is a local response, and so because offshore winds often flow either towards or parallel to the coasts of India, there are many areas where 100-m wind speed is quite high very near to the coastline. As in northern Europe, therefore, India could benefit considerably from harnessing offshore wind energy, particularly

with new developments in floating wind farm technology, which reduce requirements of shallow sea-beds. This results in many regions of offshore interest, although these must be confined to being relatively near the coast, to avoid the bathymetry becoming too deep to build turbines.

Most places along the coast have relatively high wind capacity factors—indeed they are mostly higher than the best values over any Indian land. The highest annual values, exceeding 0.4, are to be found off the coast of Gujarat and east central India (Andhra Pradesh and Odisha). If we again want to diversify to locations with good production potential outside of the monsoon, installations should be spread across the west coast of central and northern India (high in winter); the east coast of north India (i.e., Odisha and West Bengal; high in the pre-monsoon), where weak barrier flow westerlies along the Himalayan orography interact with the developing monsoonal jet; and the east coast of southern India (i.e., Tamil Nadu and Andhra Pradesh; high in the post-monsoon) when the so-called 'northeast' or 'winter' monsoon is established.

The one region that stands out as particularly excellent for offshore wind production is the Gulf of Mannar, which has a wind capacity factor greater than 0.4 in each season, with an annual average of over 0.6. This makes it among the most productive regions in the tropics, alongside the Gulf of Mexico (Canul-Reyes et al., 2022). Winds here are channelled between the orography at the southern end of the Western Ghats in southwest India and the Central Highlands of Sri Lanka, and maintain a consistently high speed all year round.

When setting up the model to represent the existing wind farm fleet, we note that wind production (Figure 5a) has a strong seasonality, ranging from an average of about 5 GW during the winter and pre-monsoon to about 12 GW during the monsoon. There is very large day-to-day variability in wind production, much more so than for solar or hydropower, but this is consistent with renewable production in other countries (Bloomfield, Brayshaw, et al., 2022; Bloomfield, Wainwright, et al., 2022; Pfenninger & Staffell, 2016; Staffell & Pfenninger, 2016). This means that, for example, during the 2021 monsoon, mean daily output for the whole of India ranged from 3.1 GW (22 August) to 22.5 GW (27 July). Figure 5 also shows a regional breakdown of reported daily production. Modelling on the sub-national level is left for future work, but we include the published numbers here for the reader's interest. As expected from the results discussed in Section 2.4, the majority of the contribution comes from the southern and western parts of India.

## 3.2 | Solar

The climatological annual mean of downward shortwave radiation at the surface (Figure S3) varies considerably across India, ranging from 125 W $m^{-2}$ in the northeast to 271 W $m^{-2}$ in the northwest. Surface shortwave radiation is generally quite low over much of the country because despite its position near the equator, India often has considerable cloud cover, which we will discuss shortly.

The similarity between the energy source (shortwave radiation at the surface) and capacity factor (Figure 7) is not as high for solar as it was for wind energy. This is because the efficiency of solar panels is inversely proportional to temperature (Equation 3). This scaling is problematic in northwest India, where regions with very high annual shortwave radiation (primarily Gujarat and Rajasthan) have only middling solar capacity factors on account of their hot climate, as 2-m temperature there can exceed 45°C in the pre-monsoon (Figure S4). In addition, solar capacity factors are generally much lower than those for to wind because solar panels can only generate power during daylight hours.

As a result, solar capacity factor varies vary little across India, where it almost invariably falls between 0.18 and 0.22. It is only significantly less than this in the perpetually cloudy northeastern states, particularly along the foothills of the eastern Himalaya, and only significantly more along the western Himalaya and Ladakh in northern India. In fact, Ladakh and Uttarakhand are the only two states where solar capacity factor exceeds 0.3 in any season, because they are cool and largely cloud-free during the pre-monsoon and monsoon seasons. However, these regions are at a high altitude and have complex terrain, which makes installation and maintenance of panels challenging—the latter being particularly important here due to considerable snowfall during the winter. These same problems also hold for the Tibetan Plateau.

However, we can leverage the fact that solar capacity is relatively uniform across India to explore strategies that distribute power generation over as much of the annual cycle as possible. Even before we consider this, there are two advantages to implementing solar: first, solar capacity is weakest during the monsoon season when wind capacity factor is by far at its highest, meaning the two complement each other to an extent; second, solar capacity factor is highest during the pre-monsoon, which, as we discussed earlier, is the hottest part of the year and thus sees the greatest power demand. The low values during the summer monsoon are due to widespread heavy cloud cover, both from convection within the monsoon as well as the larger, more organized monsoon LPSs. Low values of solar capacity factor over north India and much of Pakistan during the winter and post-

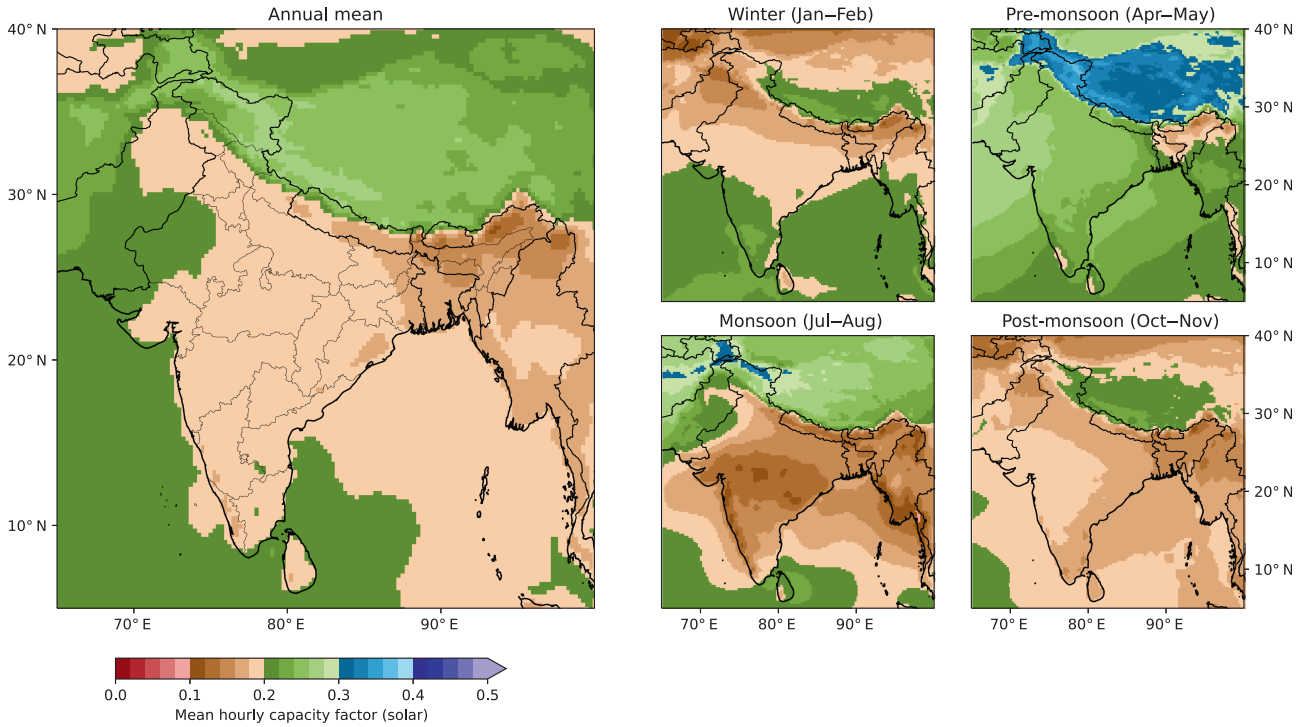


**FIGURE 7** Mean hourly solar capacity factor over India and the surrounding region from 1979 to 2020. The large panel on the left shows the annual mean as well as the state boundaries within India. The four smaller panels on the right show seasonal means of the same field.

monsoon seasons are caused by western disturbances, which are associated with extended periods of heavy cloud cover, particularly from cirrus clouds (Rao & Rao, 1971). Similarly, low values over south and south-east India are due to heavy cloud cover and rainfall associated with the northwest winter monsoon.

During the monsoon, the northwest (e.g., Rajasthan) has the highest solar capacity factor as it sits largely outside of the monsoon trough and is thus less cloudy than the rest of the subcontinent. During the post-monsoon, solar capacity factor is generally poor throughout the subcontinent, because not only does the sun have a lower zenith angle, but much of India remains cloudy after the withdrawal of the monsoon. The best regions in the post-monsoon are the far north (Ladakh and Jammu and Kashmir) and parts of the central west (e.g., Maharashtra, Gujarat and Madhya Pradesh), both of which have less cloud cover than the rest of the country. In winter, the south is largely cloud-free and so despite the lower solar zenith angle, states like Kerala and Karnataka have reasonably high solar capacity factors. During the pre-monsoon, despite the high temperatures, the northwest (e.g., Gujarat and Rajasthan) remains the best region.

When setting up the model to represent the existing solar farm developments across the continent (Figure 5b), we see considerably less variability in solar power than in wind power, though still as much as 20% difference on consecutive days. Existing solar production peaks during the pre-monsoon (March to May), in agreement with the analysis in this section. As with wind, the majority of solar production comes from the southern part of India; however, the contribution from the northern region has increased significantly in the last year with increasing investment in solar capacity there.

## 3.3 | Summary

In the previous subsections, we discussed the seasonal and spatial variability of wind and solar capacity factors. Complementary, though more simplistic, analysis for hydropower, wave power and biomass is given in Supplementary Sections 3–5, respectively. Given the breadth of material covered, we briefly summarize and inter-compare the major production areas in Figure 8. We only consider the annual mean capacity factor or energy density, as solutions to diversify against seasonality are discussed in the complementarity section later. We require that offshore wind installations are within 250 km of the coast for maintenance and ease of connection to the grid (Kucuksari et al., 2019). Given the wide range of floating and anchored turbines now available

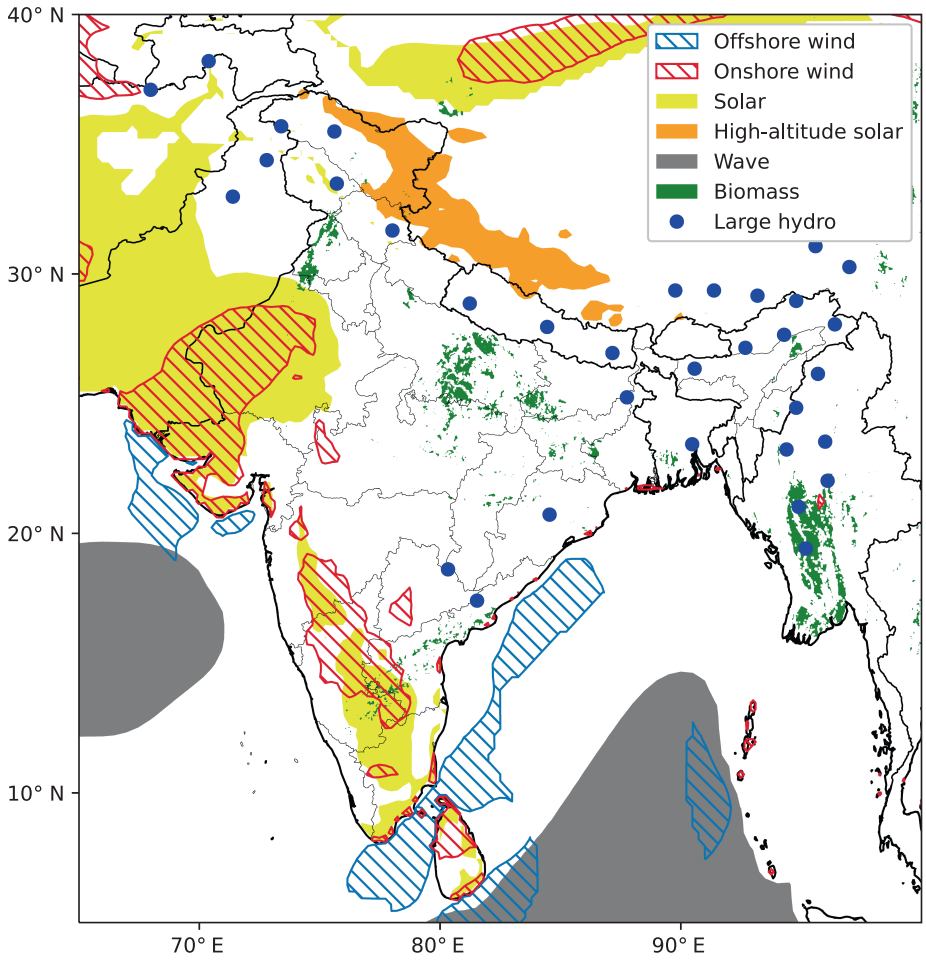


**FIGURE 8** Map showing the optimal regions for the development of new renewable energy installations over India and the surrounding region. Regions are marked as follows. Offshore wind (blue hatching): within 250 km of the coast, over the ocean and with mean wind capacity factor above the 80th percentile (~0.4). Onshore wind (red hatching): over land, surface elevation less than 2000 m, with mean wind capacity factor above the 85th percentile (~0.2). Solar (yellow): over land, surface elevation less than 3000 m, with mean solar capacity factor above the 70th percentile (~0.2). High-altitude solar (orange): over land, surface elevation greater than 3000 m, with mean solar capacity factor above the 90th percentile (~0.25). Wave (grey): mean wave energy flux above the 75th percentile (~15 kW $m^{-1}$). Biomass (green): land type must be crop, grass, shrub or herbaceous with at least 50% tree cover in at least one neighbouring 500-m grid box. Large hydro (blue circles): the 35 locations with highest maximum theoretical hydraulic power, not within 150 km of each other.

(Micallef & Rezaeiha, 2021), we do not impose a bathymetry limit here as in Figure 6, but note that the suitable locations off the coasts of Gujarat and Tamil Nadu have an ocean depth less than 200 m.

We differentiate between low-altitude and high-altitude solar to reflect the challenges associated with installing and maintaining the latter, while recognizing that these locations have some of the highest solar capacity factors in the subcontinent. Our findings are listed below.

- The best locations for offshore wind are found off the coast of Gujarat, in the Gulf of Mannar, and along much of the southeast coast of India. In many places, these regions conveniently extend very close to the coast, where the bathymetry would be shallow enough to allow them to be built on the seafloor (Canul-Reyes et al., 2022).
- The best locations for onshore wind are found over the Rann of Kutch (i.e., western Gujarat and western Rajasthan) and along the peaks of the Western Ghats. A number of very good coastal locations also emerge at this threshold, including much of the long coastlines of Tamil Nadu and Andhra Pradesh. The Andaman and Nicobar Islands also have high wind capacity factor due to their location in the opening of the Bay of Bengal.
- The best low-altitude locations for solar are in the northwest (Gujarat and Rajasthan) and south (mostly over Tamil Nadu and Karnataka) of India. These locations are often co-located with good locations for onshore wind, but as we have seen, the locations are usually associated with different seasons and weather patterns.
- High-altitude solar generally has higher capacity factors than low altitude, but comes with installation and maintenance challenges. The best locations are in Ladakh and Himachal Pradesh, as they contain the only relatively cloud-free regions during the summer monsoon.
- The best locations for large hydro (see Supplementary - Section S2.1) are largely concentrated along the Himalayas, with a few sites in the Godavari and Krishna basins in east India. Of particular interest, Arunachal Pradesh has some of the best locations for large hydro, although it currently only accounts for 1% of India's installed capacity (see Table B1).

- Wave energy (see Supplementary Section S2.2) is only really useful for the Andaman and Nicobar Islands; elsewhere, the potential is not high enough near the coast to be tapped without complex infrastructure changes. However, it does have potential to be very helpful for the Andaman and Nicobar Islands, as they are not connected to the main Indian grid and so need to produce their own energy.
- There are good opportunities for growing tree biomass (see Supplementary Section S2.3) in the north (particularly Uttar Pradesh, as well as parts of Bihar and Punjab) with small suitable regions in the south (mainly in Andhra Pradesh). For an explanation on how potentially productive regions for tree biomass are identified, see Section 1 of the Supplementary Material.

## 4 | APPLICATIONS

In this section, we explore the implications of the analysis so far—specifically the variability of solar and wind capacity factors and installation density—using our renewable production models to identify present vulnerabilities in the renewable grid and strategies for remedying them. These vulnerabilities are determined subject to three optimization criteria:

1. Maximizing local complementarity, thereby reducing the need for long transmission lines or storage solutions within the grid.
2. Reducing production seasonality, thereby reducing the need to fill long periods of extreme deficit production each year with fossil fuels.
3. Maximizing the gain in production per unit density of new installed capacity.

We now discuss each of these in turn.

### 4.1 | Maximizing local complementarity

Firstly, we look at local complementarity. We use the complementarity coefficient, defined for each grid point as $-r$, where $r$ is the linear correlation coefficient between the full wind and solar capacity factor daily mean time series, as this is highlighted as the metric most commonly used in the literature (Jurasz et al., 2020). Therefore, where the two time series are inversely correlated—and seasonal surpluses in one compensate for seasonal deficits in the other—the complementarity coefficient tends to 1. Similarly, where the two capacity factor time series are well correlated and thus seasonal deficits and surpluses tend to occur at the same times of year (which is undesirable), the complementarity coefficient tends towards −1.

Figure 9 shows a map of the complementarity coefficient for wind and solar capacity factors across India and the surrounding region. We also highlight the annual cycle and variability of the two capacity factors for eight large Indian cities in different regions. In general, complementarity is positive in the south—particularly in the southwest and south central parts of the peninsula—and negative in the north. This agrees with previous results of Nyenah et al. (2022) who only used ERA5 data from 2011 to 2020 to assess global renewable complementarity.

The reason for the positive complementarity in the south can be seen in the annual cycles at Trivandrum (complementarity coefficient over the full dataset of 0.37), Mumbai (0.69) and Hyderabad (0.53). Here, wind speed and solar radiation are inversely correlated during the monsoon, which is associated with strong near-surface winds and very cloudy conditions in this region, and outside of the monsoon, during which weak near-surface winds and clear sky conditions dominate. Chennai is an exception because it is on the leeward side of the Western Ghats, so it is often slightly drier (and so less cloudy) during the summer monsoon and considerably less windy than the west coast. Northern cities, for example, Delhi (−0.66) and Jodhpur (−0.40), diverge from this pattern. Even though they have a similar annual cycle of solar radiation, they are less windy during the monsoon because they are often further in land and usually sit inside the monsoon trough, where lower-tropospheric winds are climatologically much weaker. This means both wind and solar capacity factors are normally highest in the pre-monsoon (as shown in Sections 3.1 and 3.2).

The main implication of this is that transition to a highly renewable-based grid would be easier in the south, where wind and solar complement each other, than in the north where they co-vary over the annual cycle. Thus, where grid development is limited by transmission or storage constraints, our complementarity analysis dictates that increasing renewable capacity in the south and centre of India would have higher benefits to local cities and towns than equivalent development in the north. We note that this study does not consider land use constraints for the wind and solar PV generation, which may significantly impact this co-location potential (Deshmukh et al., 2019).

### 4.2 | Extreme surplus and deficit generation

We now consider the Indian grid as a whole, assuming that transmission attenuation is negligible. What would

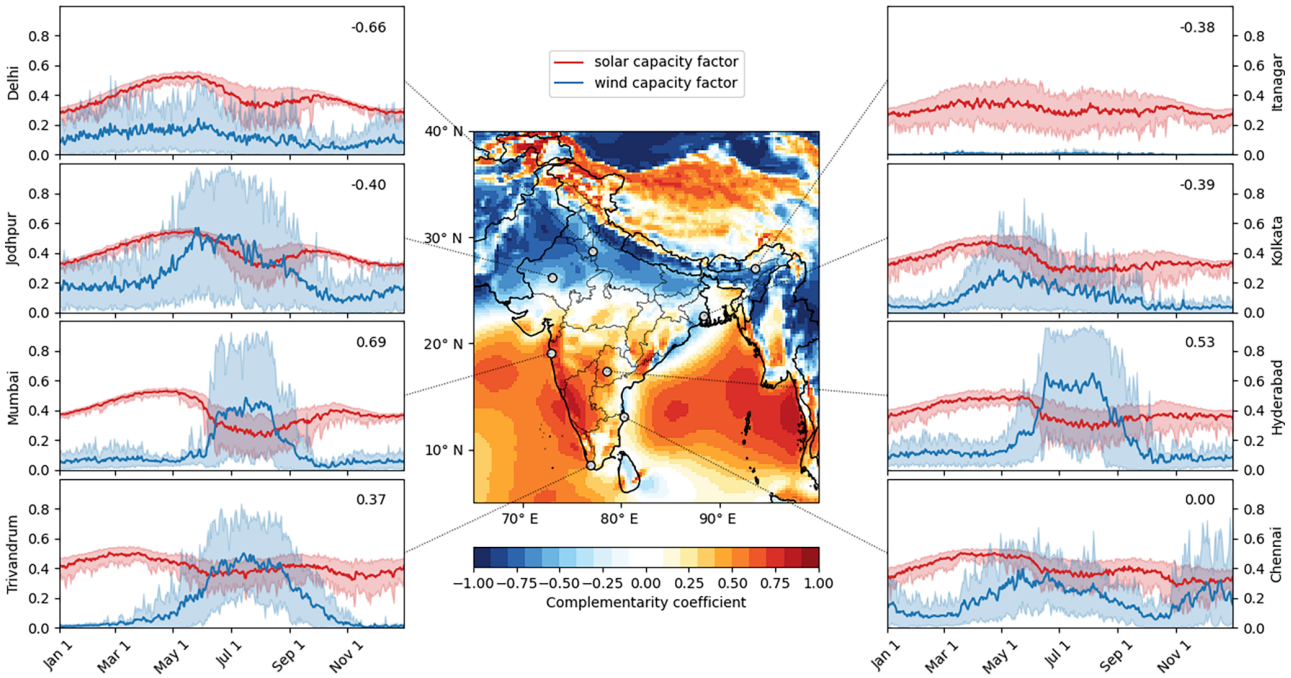


**FIGURE 9** Map of the complementarity of wind and solar capacity factor over India and the surrounding region, computed using daily mean values. Side panels show the mean annual cycle for solar (red) and wind (blue) capacity factors and complementarity coefficients (upper right; computed over the full time series) for eight cities, representing different climactic regions across India. The shaded regions in the side panels indicate the 10th and 90th percentiles. For clarity, all values of solar capacity factor are doubled. Data derived from ERA5 fields, 1979–2020.

the historical vulnerabilities of this grid be, if it were comprised of present-day wind and solar installations? We consider extremes, that is, days where renewable production would be highly deficit (below the 1st percentile) or highly surplus (above the 99th percentile). We identify such days by taking the present-day installed capacity estimates of wind and solar, computed in Section 2.4 and verified in Section 2.5. We then subject them to historical weather conditions from 1979 to 2022 and take a weighted mean (as in Section 2.5) to create an estimate for the total renewable generation (excluding hydropower) that would have occurred had the current installed capacity been in place for the last 40 years.

Figure 10 shows the locations of these deficit (yellow) and surplus (grey) days as a function of the annual cycle, against a background of the full time series of production. The full time series has the expected seasonality, albeit with substantial day-to-day variability, peaking at an average of about 25 GW during the pre-monsoon and monsoon, with much lower values (averaging 10–15 GW) in the rest of the year.

All surplus days occur between May 1 and August 9, that is, between the late pre-monsoon/early development of the monsoon onset and the height of the monsoon. Only a few surplus days occur in isolation, many are in consecutive sequences, or clusters, of three or four. The longest cluster (late June 1984) has nine consecutive surplus days. This persistence is useful because it offers predictability, meaning the grid can prepare in advance for an incoming surplus of renewable energy, and also provides an opportunity to refill depleted storage facilities. Identifying the weather patterns responsible for both isolated and clustered surplus days is left for future work. By definition, surplus days occur at a rate of 3.7 per year and have a negative trend of 0.06 days per year (or 1 day per 16 years) over the length of the dataset, but this is not significant at the 95% confidence level ($p = 0.15$).

Deficit days are more spread out, ranging from August 5 to February 3, although the majority occur in November and December. This is despite the considerable day-to-day variability within the monsoon itself. Like surplus days, most deficit days occur in clusters, ranging from 2 to 7 days in length (the longest occurring in early November 2010), although there are many broken clusters of greater length. Again, the presence of clusters offers potential predictability, especially if the responsible weather regimes are understood, and hence the opportunity for mitigation. There is an insignificant positive trend ($p = 0.8$) in deficit days of about 0.01 days per year.

Decomposing these into contributions from solar and wind production (Figure S6), we find that extreme

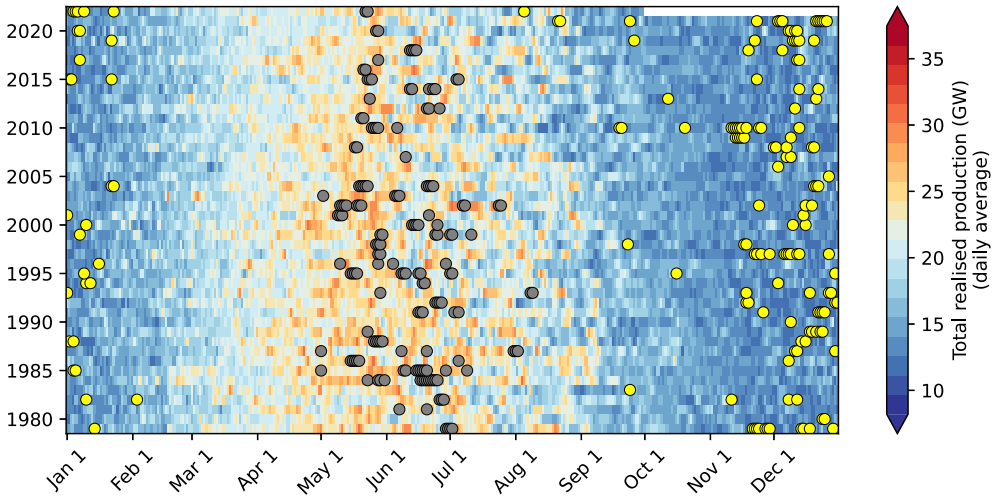


**FIGURE 10** Total wind and solar production if the present-day installed capacity were exposed to historical meteorological conditions. For each day (1979–2022), current wind and solar installation densities are multiplied by their respective mean daily capacity factors and summed to give an average output for India. Grey circles mark surplus production days (greater than 99th percentile) and yellow circles mark deficit production days (less than 1st percentile).

deficient wind days, which almost all occur from October to December, have increased insignificantly since 1979 (0.04 days per year, $p = 0.29$), whereas extreme surplus days, which all occur during the summer monsoon have insignificantly decreased during the same period (0.06 days per year, $p = 0.07$). Extreme surplus solar days, occurring predominantly in April and May, have seen an insignificant decrease since 1979 (0.04 days per year), which may be in part due to increasing pre-monsoon temperatures reducing solar panel efficiency. Extreme deficit solar days, occurring mostly in July and August, have significantly increased ($p = 0.01$) at a rate of 0.12 days per year. Determining the causes of these trends is left for future research.

The key result here is that the renewable grid, as currently installed, is vulnerable to some particular type of weather prominent in November, which can result in very low production, sometimes for several weeks at a time. Again, we leave investigation of the responsible weather conditions for future work, but it will be key to understand these weather conditions for the operation of highly renewable future Indian energy grids. In the following analysis, we explore potential ways to make the Indian renewable grid more resilient to post-monsoon and winter weather.

## 4.3 | Improving grid robustness

Finally, we investigate where new solar and wind installations should be focused to optimize production, especially in the low-production winter months. In Figure 11, we consider three such strategies: offshore wind, winter-focused onshore wind and winter-focused solar. For comparison, we also include the present-day installed wind and solar capacities, all shown as a mean annual cycle if the grid element were exposed to weather conditions from 1979 to 2020 (as in Section 4.2).

For the proposed winter-focused onshore wind, we identify the ten $1° \times 1°$ grid boxes over Indian land with the highest mean wind capacity factor between October 1 and December 31 1979–2020. Most of these are along the Pakistan border in western Gujarat and Rajasthan (i.e., the Rann of Kutch), with several in northeast Ladakh (which is impacted in the winter months by western disturbances) and coastal south Tamil Nadu (where the northeast winter monsoon winds hit the coast). These locations are consistent with wind capacity factor hotspots in the post-monsoon and winter seasons in Figure 6. If wind farms were to be installed at a density of 2 GW per grid box (which is slightly less than the present-day density over the Western Ghats, see Figure 3), that is, to a total installed capacity of 20 GW, the mean annual cycle of their total output would be given by the solid blue line in the left panel of Figure 11. Production during the winter and pre-monsoon (November through early May) is comparable to that produced by the existing installed wind, whose installed capacity is more than twice as high. This distribution therefore represents a plausible pathway to reducing the strong seasonality of onshore wind power in India. It also helps to increase the complementarity with solar PV shown in in Figure 10.

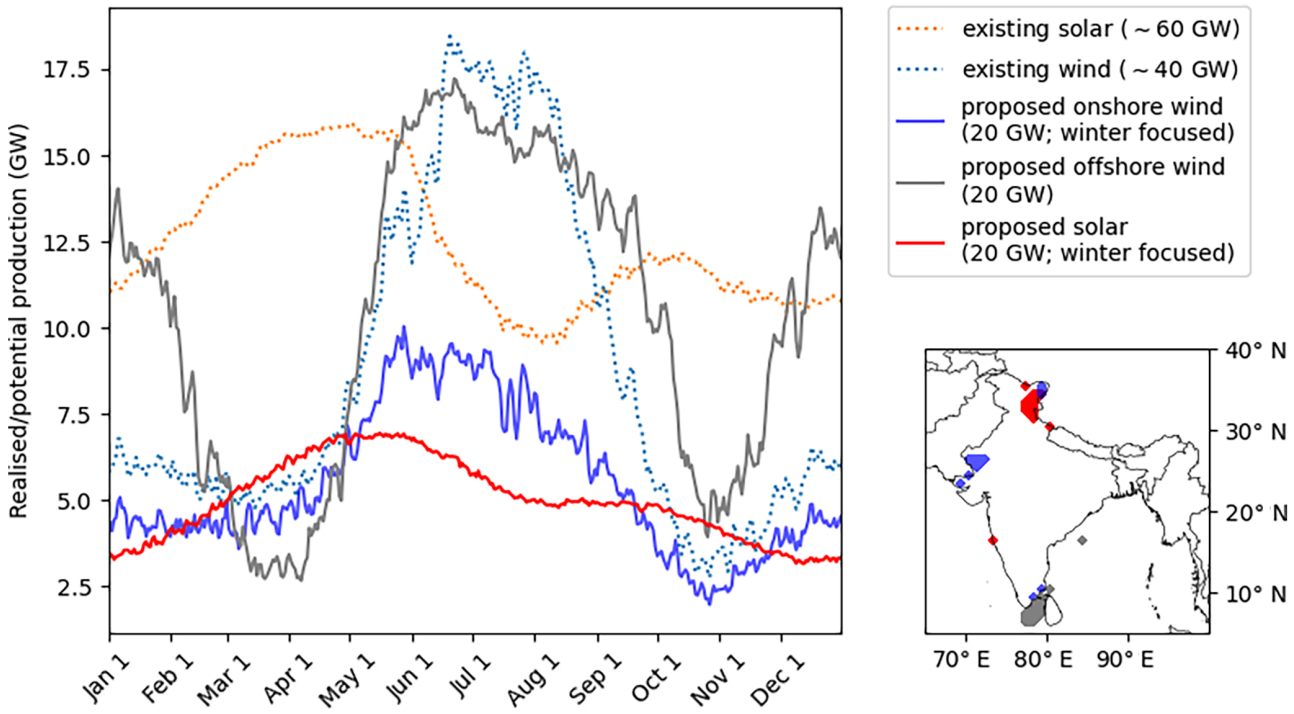


**FIGURE 11** Mean annual cycle of the output of existing solar (dotted orange) and existing wind (dotted blue) installations if they were exposed to historical weather conditions from 1979 to 2020. We also show the annual cycle of output, computed in the same way, for three proposed installations (marked on the map, lower right): 20 GW of offshore wind (grey) and 20 GW of onshore wind (blue) and solar (red), each seeking to maximize output during the post-monsoon and winter months. Proposed installations have a density of 2 GW per $1° \times 1°$ grid box, distributed equally over an area equal to 10 such grid boxes.

For the proposed winter-focused solar, we follow the same method as above. We impose no additional criterion for altitude, as we did in Figure 8. All except one of the ten optimal grid boxes are along the western Himalaya: in Ladakh, Himachal Pradesh and Uttarakhand. This is hardly surprising, because this is the sunniest region in India in each of the four seasons (Figure 7). There is also a single grid box highlighted on the west coast of Maharashtra, far enough north to avoid cloudiness associated with the northeast monsoon and far enough south to retain a reasonable solar zenith angle in the winter. This set-up provides slightly more production per installed unit of capacity than the present-day installed solar. Gaining more than this is difficult given the homogeneity of solar capacity factor over India (Figure 7). The seasonality is also very slightly reduced as clouds associated with the summer monsoon seldom penetrate as far as eastern Ladakh, nor to the high altitudes of the western Himalaya. However, the gains in each case are small, and probably not worth the logistic complexities of installing and maintaining high-altitude solar panel installations. In short, seasonal shortfalls in solar production cannot be fixed by redistributing solar panels, rather we must rely on complementarity with wind power.

For the proposed offshore wind, we use a slightly different method to the two cases above. First, we drop the winter constraint, instead finding grid boxes that maximize mean capacity factor over the whole year. Second, we apply offshore criteria: that the grid boxes must be over the ocean, but must also be within 250 km of the coastline. This latter restriction largely keeps the bathymetry from being too deep to permit installation, and ensures that the required length of transmission is not too large (Kucuksari et al., 2019). Eight of the ten most optimal grid boxes are in the Gulf of Mannar, with one of the remaining two located just on the other side of the Palk Strait. This is unsurprising in the context of Figure 6, where we saw that this region has by far the highest climatological wind power generation of anywhere in the subcontinent. These winds are particularly strong in both the summer and northeast winter monsoons. The remaining optimal grid box, situated off the coast of Andhra Pradesh, receives strong winds during the monsoon as well as the pre- and post-monsoon seasons. These offshore regions are in fact so productive—with an annual mean capacity factor often exceeding 50%—that this proposed 20 GW installation would produce an average output of 10.4 GW, about 20% higher than the existing present-day installed wind (whose

installed capacity is over 40 GW). Therefore, there is clearly a benefit to investing in offshore wind, notwithstanding the increased cost over onshore installation, as many other countries in particularly windy areas of the planet have already done (e.g., the United Kingdom; Drew et al., 2015). The other key benefit of this proposed offshore wind installation is that it can take advantage of the winter northeast monsoon, resulting in very high production in December, January and much of February. With solar then able to compensate for weaker production in November and March, this is possibly the only realistic solution to reduce the seasonality of renewable energy production in India.

We note that this is a simplistic and purely meteorological analysis, and we do not take into account installation or transmission costs, population density or current land use. Readers should also be aware that limitations in the ERA5 input data (biases and relatively coarse resolution) will lead to uncertainty in the results presented here.

## 5 | DISCUSSION AND CONCLUSIONS

In this article, we presented a complete inventory of potential and realized renewable energy capacity over India. This was broadly separated into three main tasks: quantifying the spatial distribution of existing renewable energy capacity; estimating historical renewable capacity factors; combining these into a model to identify strengths and weaknesses of the existing grid; and to propose solutions to the latter going forward.

### 5.1 | Potential capacity

We used data from ERA5 and various land use datasets to quantify the most potentially productive regions for each type of renewable:

- The best location for offshore wind is found in the Gulf of Mannar, on the southern tip of the Indian peninsula. It has such a high annual mean wind capacity factor that it is one of the best locations in the tropics for an offshore wind installation. Other good locations are off the coast of Gujarat and along the southeast coast of India. The highest wind capacity factor in each of these locations occurs during the summer monsoon (July–August). These locations are all sufficiently close to the coast that they could support either fixed foundation or floating wind turbines.
- The best locations for onshore wind are found over the Rann of Kutch (i.e., western Gujarat and western Rajasthan) and along the peaks of the Western Ghats. Wind capacity factor peaks during the monsoon for almost all locations over peninsula India, although it extends into the pre-monsoon (April–May) for the Rann of Kutch.
- Mean solar capacity factor varies little over most of India. However, the best low-altitude (<3000 m) locations for solar are in the northwest (Gujarat and Rajasthan) and south (mostly over Tamil Nadu and Karnataka). Solar capacity factor is highest during the pre-monsoon for all of India, except some parts of the southwest (e.g., Kerala), where it peaks during winter (January–February).
- High-altitude locations (>3000 m) generally have higher solar capacity factors than low-altitude locations, although installations in these regions can be difficult to maintain. The best locations are in Ladakh and Himachal Pradesh, which benefit from being cloud free during both the pre-monsoon and monsoon.
- Wave energy potential is typically weak near the Indian coasts. An important exception to this is the Andaman and Nicobar Islands, for whom it could be beneficial as they are not connected to the main Indian power grid. Wave energy potential is largest, by far, during the summer monsoon.
- A qualitative examination of large hydropower potential showed that most of the best locations are located along the Himalayas, given the large head available there. This includes Arunachal Pradesh, which currently has very little installed hydropower capacity. Other potential areas of interest included the Godavari (namely Odisha) and Krishna (Telangana and Andhra Pradesh) river basins. Similar analysis of small (i.e., run of river) hydropower potential identified tributaries of the Ganges and Brahmaputra as good locations. Potential hydropower production is highest during the monsoon for virtually the entire subcontinent.

The focus of this analysis has been understanding renewable potential and variability using the ERA5 reanalysis. ERA5 has previously been found to be the best performing reanalysis over India when compared with buoy data from the open ocean, but near-surface wind speed is notably more poorly represented than temperature or sea level pressure (Luo et al., 2022). The open ocean is significantly less challenging for the reanalysis than a region of complex orography, such as the Western Ghats, where the majority of the Indian wind farms are located. Previous studies have highlighted ERA5's issues over orography (Bloomfield et al., 2020) and the potential need for calibration to a product such as the Global Wind Atlas (Davis et al., 2023) or for regional high-resolution

reanalysis (e.g., the Indian Monsoon Data Assimilation Analysis [IMDAA]; Ashrit et al., 2020). Very little is provided on the verification of surface radiation fields over India. However, there is information about precipitation.

In this study, we chose to use an uncorrected ERA5 to demonstrate the methodology and to allow us to freely discuss the complementarity between renewables (Figure 9 and related analysis) without worries that the correction of wind speed had impacted the relationship between near-surface winds and surface solar radiation. However, it is still possible that biases in ERA5 wind speeds could impact the complementarity of renewables seen in Figure 9. This could be particularly problematic for proposed wind farms in mountainous regions.

## 5.2 | Installed capacity

We used a combination of catalogue data, satellite data and OpenStreetMap data to estimate the existing spatial capacity density of wind and solar installations. We then verified our results using state-wide totals published by the Ministry for New and Renewable Energy. All sources were generally in agreement.

## 5.3 | Modelling grid resilience

We combined historical capacity factor time series with gridded estimates of installed capacity to produce a model for simulating renewable energy production over India. We used this model for two key purposes: first, to identify periods of deficit and surplus renewable production were the present-day grid exposed to historical weather conditions; and second, to establish potential regions for new renewable installations that might help to address identified weaknesses in the existing grid. Our model performed well over a testing period (January 2020 to October 2022), with simulated daily mean wind and solar production having correlation coefficients of 0.922 and 0.951, respectively, with published values. However, our simple model does not represent changes in the spatial distribution of installed capacity, and so its skill is weakened as a result.

By subjecting the present-day renewable grid to historical weather conditions (1979–2020), we demonstrated that there is a strong seasonality, with mean production during the monsoon reaching about 30 GW compared with 10–15 GW during the winter. Production during the monsoon is primarily wind-driven and is thus highly variable. Extreme deficit days (where grid production is below the first percentile) typically occur during November and December, and often happen consecutively in clusters that can be over a week long, offering some predictability.

Extreme surplus days (production greater than the 99th percentile) typically occur between late May and early August, and similarly are often found in clusters. Neither extreme surplus nor extreme deficit days have significant trends in frequency over this period, so although both wind (increase in deficit) and solar (increase in deficit and decrease in surplus) have significant trends individually, the current arrangement of the renewable grid is somewhat shielded from the recent effects of climate change.

In the final part of this study, we used the model to identify regions where new wind and solar installations should be located to maximize the following: offshore wind production, onshore wind production during winter and solar production during winter. We showed that 20 GW of offshore wind installed capacity, located primarily in the Gulf of Mannar, would produce approximately the same amount of power as the existing onshore wind installations, which total a nominal capacity of over 40 GW. We also showed that winter-focused solar and onshore wind installations, designed to mitigate the strong seasonality in production exhibited by the existing renewable grid, should be primarily located in Ladakh/Himachal Pradesh and Rajasthan/Ladakh, respectively.

This study supports relevant work investigating the predictability of weather-dependent energy system components. At short lead-times methods are being developed to nowcast solar PV generation using satellite data (Masoom et al., 2020). At sub-seasonal to seasonal timescales, although there is limited model skill, predictability is highest over the southern regions of the country (Das & Baidya Roy, 2021) where our study has highlighted the largest renewable complementarity.

## 5.4 | Open data

Table 1 gives a summary of the data produced by this study. All other data are available from sources stated, for example, in Section 2 or in figure captions. Code used to produce the data and figures in this article is available at https://github.com/kieranmrhunt/india-renewable.

## 5.5 | Future work

We did not assess any long-term trends present in the reanalysis data (e.g., the potential for steady wind speed decline in the monsoon season; Gao et al., 2018). Nor did we assess the potential impacts of climate change on wind and solar PV generation over India (e.g., those

discussed in Zakari et al., 2022), which would provide useful extensions of the wind and solar capacity datasets developed in Section 3 to understand whether the trends seen in extreme wind/solar days in Figure 10 are a result of inter-annual variability, or the impact of climate change. There is also a clear need to identify the weather patterns responsible for these extreme days, and to understand its potential predictability from days to months ahead.

In addition to understanding the impact of climate change, another important consideration for future work is the evolution of energy demand (e.g., scenarios described in Barbar et al., 2021), which will grow substantially through India's decarbonization.

## AUTHOR CONTRIBUTIONS

**Kieran M. R. Hunt:** Conceptualization (equal); data curation (lead); formal analysis (lead); investigation (equal); methodology (supporting); resources (supporting); visualization (lead); writing – original draft (lead); writing – review and editing (equal). **Hannah C. Bloomfield:** Conceptualization (equal); data curation (supporting); formal analysis (supporting); investigation (equal); methodology (lead); resources (lead); visualization (supporting); writing – original draft (supporting); writing – review and editing (equal).

## ACKNOWLEDGEMENTS

Kieran M. R. Hunt is supported by a NERC Independent Research Fellowship (MITRE; NE/W007924/1). Hannah C. Bloomfield was funded by the Natural Environment Research Council as part of the UK Centre for Greening Finance and Investment (NERC CGFI 736 Grant Number NE/V017756/1). Kieran M. R. Hunt does not wish to thank the journal *Meteorological Applications*, whose officious approach to manuscript submission was most obstructive.

## DATA AVAILABILITY STATEMENT

All data and code used in this paper are freely available at https://doi.org/10.5281/zenodo.7824872 and https://github.com/kieranmrhunt/india-renewable respectively.

## ORCID

*Kieran M. R. Hunt* https://orcid.org/0000-0003-1480-3755

*Hannah C. Bloomfield* https://orcid.org/0000-0002-5616-1503

## REFERENCES

Ashrit, R., Indira Rani, S., Kumar, S., Karunasagar, S., Arulalan, T., Francis, T. et al. (2020) IMDAA regional reanalysis: performance evaluation during Indian summer monsoon season. *Journal of Geophysical Research: Atmospheres*, 125(2), e2019JD030973.

Barbar, M., Mallapragada, D.S., Alsup, M. & Stoner, R. (2021) Scenarios of future Indian electricity demand accounting for space cooling and electric vehicle adoption. *Scientific Data*, 8(1), 178.

Beck, H.E., Zimmermann, N.E., McVicar, T.R., Vergopolan, N., Berg, A. & Wood, E.F. (2018) Present and future Köppen-Geiger climate classification maps at 1-km resolution. *Scientific Data*, 5(1), 1–12.

Bett, P.E. & Thornton, H.E. (2016) The climatological relationships between wind and solar energy supply in Britain. *Renewable Energy*, 87, 96–110.

Bloomfield, H., Gonzalez, P.L., Lundquist, J.K., Stoop, L.P., Browell, J., Dargaville, R. et al. (2021) The importance of weather and climate to energy systems: a workshop on next generation challenges in energy–climate modeling. *Bulletin of the American Meteorological Society*, 102(1), E159–E167. Available from: https://doi.org/10.1175/BAMS-D-20-0256.1

Bloomfield, H.C., Brayshaw, D.J. & Charlton-Perez, A.J. (2020) Characterizing the winter meteorological drivers of the European electricity system using targeted circulation types. *Meteorological Applications*, 27(1), e1858.

Bloomfield, H.C., Brayshaw, D.J., Deakin, M. & Greenwood, D. (2022) Hourly historical and near-future weather and climate variables for energy system modelling. *Earth System Science Data*, 14(6), 2749–2766.

Bloomfield, H.C., Brayshaw, D.J., Shaffrey, L.C., Coker, P.J. & Thornton, H. (2016) Quantifying the increasing sensitivity of power systems to climate variability. *Environmental Research Letters*, 11(12), 124025. Available from: https://doi.org/10.1088/1748-9326/11/12/124025

Bloomfield, H.C., Wainwright, C.M. & Mitchell, N. (2022) Characterizing the variability and meteorological drivers of wind power and solar power generation over Africa. *Meteorological Applications*, 29(5), e2093.

Boretti, A. & Castelletto, S. (2020) Cost of wind energy generation should include energy storage allowance. *Scientific Reports*, 10(1), 1–13.

Canul-Reyes, D.A., Rodrguez-Hernández, O. & Jarquin-Laguna, A. (2022) Potential zones for offshore wind power development in the Gulf of Mexico using reanalyses data and capacity factor seasonal analysis. *Energy for Sustainable Development*, 68, 211–219.

Curio, J., Schiemann, R., Hodges, K.I. & Turner, A.G. (2019) Climatology of Tibetan Plateau vortices in reanalysis data and a high-resolution global climate model. *Journal of Climate*, 32(6), 1933–1950.

Das, A. & Baidya Roy, S. (2021) Evaluation of subseasonal to seasonal forecasts over India for renewable energy applications. *Advances in Geosciences*, 56, 89–96.

Davis, N.N., Badger, J., Hahmann, A.N., Hansen, B.O., Mortensen, N.G., Kelly, M. et al. (2023) The Global Wind Atlas: a high-resolution dataset of climatologies and associated web-based application. *Bulletin of the American Meteorological Society*, 104(8), E1507–E1525.

Deshmukh, R., Wu, G.C., Callaway, D.S. & Phadke, A. (2019) Geospatial and techno-economic analysis of wind and solar resources in India. *Renewable Energy*, 134, 947–960.

Deshmukh, R., Wu, G.C. & Phadke, A. (2017) *Renewable energy zones for balancing siting trade-offs in India*. Tech. Rep. 1007272. Santa Barbara: UC Santa Barbara. Available from: https://doi.org/10.2172/1366450

Dhar, O.N. & Rakhecha, P.R. (1983) Foreshadowing northeast monsoon rainfall over Tamil Nadu, India. *Monthly Weather Review*, 111, 109–112.

Dimri, A.P., Niyogi, D., Barros, A.P., Ridley, J., Mohanty, U.C., Yasunari, T. et al. (2015) Western disturbances: a review. *Reviews of Geophysics*, 53(2), 225–246.

Drew, D.R., Cannon, D.J., Brayshaw, D.J., Barlow, J.F. & Coker, P.J. (2015) The impact of future offshore wind farms on wind power generation in Great Britain. *Resources*, 4(1), 155–171.

Dubus, L., Brayshaw, D.J., Huertas-Hernando, D., Radu, D., Sharp, J., Zappa, W. et al. (2022) Towards a future-proof climate database for European energy system studies. *Environmental Research Letters*, 17(12), 121001. Available from: https://doi.org/10.1088/1748-9326/aca1d3

Dunning, C., Turner, A. & Brayshaw, D. (2015) The impact of monsoon intraseasonal variability on renewable power generation in India. *Environmental Research Letters*, 10(6), 064002. Available from: https://doi.org/10.1088/1748-9326/10/6/064002

Evans, D.L. & Florschuetz, L.W. (1977) Cost studies on terrestrial photovoltaic power systems with sunlight concentration. *Solar Energy*, 19(3), 255–262.

Fasullo, J. & Webster, P.J. (2003) A hydrological definition of Indian monsoon onset and withdrawal. *Journal of Climate*, 16(19), 3200–3211.

Gangopadhyay, A., Seshadri, A.K., Sparks, N.J. & Toumi, R. (2022) The role of wind-solar hybrid plants in mitigating renewable energy-droughts. *Renewable Energy*, 194, 926–937. Available from: https://doi.org/10.1016/j.renene.2022.05.122

Gao, M., Ding, Y., Song, S., Lu, X., Chen, X. & McElroy, M.B. (2018) Secular decrease of wind power potential in India associated with warming in the Indian Ocean. *Science Advances*, 4(12), eaat5256.

Gopi, A., Sudhakar, K., Keng, N.W., Krishnan, A.R. & Priya, S.S. (2021) Performance modeling of the weather impact on a utility-scale PV power plant in a tropical region. *International Journal of Photoenergy*, 2021, 1–10. Available from: https://doi.org/10.1155/2021/5551014

Gulagi, A., Bogdanov, D. & Breyer, C. (2017) The demand for storage technologies in energy transition pathways towards 100% renewable energy for India. *Energy Procedia*, 135, 37–50. Available from: https://doi.org/10.1016/j.egypro.2017.09.485

Gulagi, A., Ram, M. & Breyer, C. (2020) Role of the transmission grid and solar wind complementarity in mitigating the monsoon effect in a fully sustainable electricity system for India. *IET Renewable Power Generation*, 14(2), 254–262.

Harrigan, S., Zsoter, E., Alfieri, L., Prudhomme, C., Salamon, P., Wetterhall, F. et al. (2020) GloFAS-ERA5 operational global river discharge reanalysis 1979–present. *Earth System Science Data*, 12(3), 2043–2060.

Hersbach, H., Bell, B., Berrisford, P., Hirahara, S., Horányi, A., Muñoz-Sabater, J. et al. (2020) The ERA5 global reanalysis. *Quarterly Journal of the Royal Meteorological Society*, 146(730), 1999–2049.

Hossain, J., Sharma, D., Mishra, N.K., Ansari, M.Z. & Kishore, V.V.N. (2016) Re-assessment of wind energy potential with new technology in India. *Wind Engineering*, 40(4), 379–397. Available from: https://doi.org/10.1177/0309524X16651176

Hunt, K.M.R., Curio, J., Turner, A.G. & Schiemann, R. (2018) Subtropical westerly jet influence on occurrence of western disturbances and Tibetan Plateau vortices. *Geophysical Research Letters*, 45(16), 8629–8636.

Hunt, K.M.R. & Fletcher, J.K. (2019) The relationship between Indian monsoon rainfall and low-pressure systems. *Climate Dynamics*, 53(3–4), 1–13.

Hunt, K.M.R. & Menon, A. (2019) The 2018 Kerala floods: a climate change perspective. *Climate Dynamics*, 54(3), 2433–2446.

Hunt, K.M.R., Turner, A.G. & Shaffrey, L.C. (2018) The evolution, seasonality, and impacts of western disturbances. *Quarterly Journal of the Royal Meteorological Society*, 144(710), 278–290. Available from: https://doi.org/10.1002/qj.3200

Indian Power Industry Investment. (2023) Renewable energy in India – Indian Power Industry Investment. Available from: https://www.investindia.gov.in/sector/renewable-energy#:~:text=India's%20installed%20renewable%20energy%20capacity,additions%20of%209.83%25%20in%202022

International Electrotechnical Commission. (2005) International Standard IEC 61400-1. Wind turbines – Part 1: Design requirements. Available from: https://webstore.iec.ch/preview/info_iec61400-1%7Bed3.0%7Den.pdf

International Hydropower Association. (2022) *Hydropower status report*. London: International Hydropower Association. Available from: https://www.hydropower.org/country-profiles/nepal

Jain, A., Das, P., Yamujala, S., Bhakar, R. & Mathur, J. (2020) Resource potential and variability assessment of solar and wind energy in India. *Energy*, 211(118), 993. Available from: https://doi.org/10.1016/j.energy.2020.118993

Jurasz, J., Canales, F.A., Kies, A., Guezgouz, M. & Beluco, A. (2020) A review on the complementarity of renewable energy sources: concept, metrics, application and future research directions. *Solar Energy*, 195, 703–724.

Kruitwagen, L., Story, K.T., Friedrich, J., Byers, L., Skillman, S. & Hepburn, C. (2021) A global inventory of photovoltaic solar energy generating units. *Nature*, 598(7882), 604–610.

Kucuksari, S., Erdogan, N. & Cali, U. (2019) Impact of electrical topology, capacity factor and line length on economic performance of offshore wind investments. *Energies*, 12(16), 3191.

Kulkarni, S., Deo, M. & Ghosh, S. (2018a) Framework for assessment of climate change impact on offshore wind energy. *Meteorological Applications*, 25(1), 94–104.

Kulkarni, S., Deo, M. & Ghosh, S. (2018b) Impact of active and break wind spells on the demand–supply balance in wind energy in India. *Meteorology and Atmospheric Physics*, 130, 81–97.

Lledó, L., Torralba, V., Soret, A., Ramon, J. & Doblas-Reyes, F.J. (2019) Seasonal forecasts of wind power generation. *Renewable Energy*, 143, 91–100.

Lu, T., Sherman, P., Chen, X., Chen, S., Lu, X. & McElroy, M. (2020) India's potential for integrating solar and on-and offshore wind power into its energy system. *Nature Communications*, 11(1), 4750.

Lugovoy, O., Jyothiprakash, V., Chatterjee, S., Sharma, S., Mukherjee, A., Das, A. et al. (2021) Towards a zero-carbon electricity system for India in 2050: IDEEA model-based scenarios integrating wind and solar complementarity and geospatial endowments. *Energies*, 14(21), 7063.

Luo, Y., Liu, L., Yang, Y., Liu, B., Yang, G., Wang, H. et al. (2022) Evaluation of meteorological reanalysis data over the tropical Western Indian Ocean based on buoy observations in 2022. *Journal of Sea Research*, 189(102), 285.

Mahtta, R., Joshi, P.K. & Jindal, A.K. (2014) Solar power potential mapping in India using remote sensing inputs and environmental parameters. *Renewable Energy*, 71, 255–262. Available from: https://doi.org/10.1016/j.renene.2014.05.037

Masoom, A., Kosmopoulos, P., Bansal, A. & Kazadzis, S. (2020) Solar energy estimations in India using remote sensing technologies and validation with sun photometers in urban areas. *Remote Sensing*, 12(2), 254.

Micallef, D. & Rezaeiha, A. (2021) Floating offshore wind turbine aerodynamics: trends and future challenges. *Renewable and Sustainable Energy Reviews*, 152(111), 696.

Mohapatra, M., Bandyopadhyay, B.K. & Tyagi, A. (2012) Best track parameters of tropical cyclones over the North Indian Ocean: a review. *Natural Hazards*, 63, 1285–1317.

Mulligan, M., van Soesbergen, A. & Sáenz, L. (2020) GOODD, a global dataset of more than 38,000 georeferenced dams. *Scientific Data*, 7(1), 31.

Muneer, T., Asif, M. & Munawwar, S. (2005) Sustainable production of solar electricity with particular reference to the Indian economy. *Renewable and Sustainable Energy Reviews*, 9(5), 444–473. Available from: https://doi.org/10.1016/j.rser.2004.03.004

Nyenah, E., Sterl, S. & Thiery, W. (2022) Pieces of a puzzle: solar-wind power synergies on seasonal and diurnal timescales tend to be excellent worldwide. *Environmental Research Communications*, 4(5), 055011.

OpenStreetMap contributors. (2017) Planet dump. Available from: https://planet.osm.org. https://www.openstreetmap.org

Pfenninger, S. & Staffell, I. (2016) Long-term patterns of European PV output using 30 years of validated hourly reanalysis and satellite data. *Energy*, 114, 1251–1265.

Phadtare, J.A., Fletcher, J.K., Ross, A.N., Turner, A.G. & Schiemann, R.K.H. (2022) Froude-number-based rainfall regimes over the Western Ghats mountains of India. *Quarterly Journal of the Royal Meteorological Society*, 148, 3388–3405.

Rajeevan, M., Unnikrishnan, C.K., Bhate, J., Niranjan Kumar, K. & Sreekala, P.P. (2012) Northeast monsoon over India: variability and prediction. *Meteorological Applications*, 19(2), 226–236.

Rao, V.B., Rao, K.K., Mahendranath, B., Lakshmi Kumar, T. & Govardhan, D. (2021) Large-scale connection to deadly Indian heatwaves. *Quarterly Journal of the Royal Meteorological Society*, 147(735), 1419–1430.

Rao, V.B. & Rao, S.T. (1971) A theoretical and synoptic study of western disturbances. *Pure and Applied Geophysics*, 90(1), 193–208.

Ratnam, J.V., Behera, S.K., Ratna, S.B., Rajeevan, M. & Yamagata, T. (2016) Anatomy of Indian heatwaves. *Scientific Reports*, 6(1), 24395.

Saidur, R., Rahim, N.A., Islam, M.R. & Solangi, K.H. (2011) Environmental impact of wind energy. *Renewable and Sustainable Energy Reviews*, 15(5), 2423–2430. Available from: https://doi.org/10.1016/j.rser.2011.02.024

Schiemann, R., Lüthi, D. & Schär, C. (2009) Seasonality and interannual variability of the westerly jet in the Tibetan Plateau region. *Journal of Climate*, 22(11), 2940–2957.

Staffell, I. & Pfenninger, S. (2016) Using bias-corrected reanalysis to simulate current and future wind power output. *Energy*, 114, 1224–1239.

Thomas, T.M., Bala, G. & Srinivas, V.V. (2021) Characteristics of the monsoon low pressure systems in the Indian subcontinent and the associated extreme precipitation events. *Climate Dynamics*, 56, 1859–1878.

Wang, J., Walter, B.A., Yao, F., Song, C., Ding, M., Maroof, A.S. et al. (2022) GeoDAR: georeferenced global dams and reservoirs dataset for bridging attributes and geolocations. *Earth System Science Data*, 14(4), 1869–1899.

Wu, X., Hu, Y., Li, Y., Yang, J., Duan, L., Wang, T. et al. (2019) Foundations of offshore wind turbines: a review. *Renewable and Sustainable Energy Reviews*, 104, 379–393. Available from: https://doi.org/10.1016/j.rser.2019.01.012

Xu, R., Zeng, Z., Pan, M., Ziegler, A.D., Holden, J., Spracklen, D.V. et al. (2023) A global-scale framework for hydropower development incorporating strict environmental constraints. *Nature Water*, 1–10, 113–122. Available from: https://doi.org/10.1038/s44221-022-00004-1

Zakari, Y., Michel, A. & Lehning, M. (2022) Future trends in wind resources and their consistency in the indian sub-continent. *Sustainable Energy Technologies and Assessments*, 53(102), 460.

Zsoter, E., Harrigan, S., Wetterhall, G., Salamon, P. & Prudhomme, C. (2019) River discharge and related forecasted data from the Global Flood Awareness System, v2.1, Copernicus Climate Change Service (C3S) Climate Data Store (CDS). https://doi.org/10.24381/cds.a4fdd6b9

## SUPPORTING INFORMATION

Additional supporting information can be found online in the Supporting Information section at the end of this article.

**How to cite this article:** Hunt, K. M. R., & Bloomfield, H. C. (2024). Quantifying renewable energy potential and realized capacity in India: Opportunities and challenges. *Meteorological Applications*, *31*(3), e2196. https://doi.org/10.1002/met.2196

## APPENDIX A: EXTRACTING OSM DATA

To extract the location data of renewable installations from OSM, we used scripts of the following format on Overpass Turbo (https://overpass-turbo.eu/):

```
[out:json][timeout:250];
// gather results
(
// query part for: "" generator:source"=wind"
node["generator:source"="wind"]({{bbox}});
way["generator:source"="wind"]({{bbox}});
relation["generator:source"="wind"]({{bbox}});
);
// print results
out body;
>;
out skel qt;
```

## APPENDIX B: STATE-WISE INSTALLED RENEWABLE POWER CAPACITY

**TABLE B1** Installed renewable power capacity in Indian states and territories as of 30 October 2022.

| State/territory | Biomass (MW) | Small hydro (MW) | Large hydro (MW) | Wind (MW) | Solar (MW) | Total (MW) | Solar (% on grid) | Solar (% rooftop) |
|---|---|---|---|---|---|---|---|---|
| Andaman and Nicobar | | 5.25 | | | 29.91 | 35.16 | 99.10 | 15.49 |
| Andhra Pradesh | **566.04** | 162.11 | 1673.60 | 4096.65 | 4506.66 | 11,005.06 | 98.04 | 3.64 |
| Arunachal Pradesh | | 133.11 | 544.55 | | 11.23 | 688.89 | 49.96 | 77.36 |
| Assam | 2.00 | 34.11 | 522.08 | | 147.92 | 706.11 | 93.62 | 24.18 |
| Bihar | 126.02 | 70.70 | 110.00 | | 190.76 | 497.48 | 88.84 | 18.03 |
| Chandigarh | | | 101.71 | | 57.84 | 159.55 | 98.60 | 88.88 |
| Chhatisgarh | 275.00 | 76.00 | 233.00 | | 798.34 | 1382.34 | 51.56 | 11.46 |
| Dadar and Nagar Haveli | | | | | 5.46 | 5.46 | 100.00 | 54.40 |
| Daman and Diu | | | | | 41.01 | 41.01 | 100.00 | 75.25 |
| Delhi | 59.00 | | 723.09 | | 211.12 | 993.21 | 99.31 | 95.73 |
| Goa | 0.34 | 0.05 | 2.00 | | 26.40 | 28.79 | 99.55 | 96.39 |
| Gujarat | 110.73 | 89.39 | 772.00 | **9798.52** | **8045.58** | **18,816.22** | 99.46 | 24.46 |
| Haryana | 258.88 | 73.50 | 2324.62 | | 954.65 | 3611.65 | 69.61 | 60.00 |
| Himachal Pradesh | 10.20 | **960.71** | **3248.88** | | 87.35 | 4307.14 | 65.72 | 33.64 |
| Jammu & Kashmir | | 144.68 | 2321.88 | | 48.56 | 2515.12 | 50.43 | 89.83 |
| Jharkhand | 4.30 | 4.05 | 191.00 | | 93.58 | 292.93 | 57.98 | 64.89 |
| Karnataka | **1902.15** | **1280.73** | **3631.60** | **5268.15** | **7859.38** | **19,942.01** | 99.61 | 4.88 |
| Kerala | 2.50 | **266.52** | 1864.15 | 62.50 | 653.97 | 2849.64 | 96.83 | 54.76 |
| Ladakh | | 39.64 | | | 7.80 | 47.44 | 100.00 | 23.08 |

(Continues)

**TABLE B1** (Continued)

| State/territory | Biomass (MW) | Small hydro (MW) | Large hydro (MW) | Wind (MW) | Solar (MW) | Total (MW) | Solar (% on grid) | Solar (% rooftop) |
|---|---|---|---|---|---|---|---|---|
| Lakshwadeep | | | | | 3.27 | 3.27 | 22.94 | 0.00 |
| Madhya Pradesh | 131.75 | 99.71 | 3223.66 | 2844.29 | 2762.14 | 9061.55 | 97.04 | 8.26 |
| Maharashtra | **2636.42** | **381.08** | **3331.84** | **5012.83** | 3391.63 | **14,753.80** | 97.05 | 36.53 |
| Manipur | | 5.45 | 87.24 | | 12.28 | 104.97 | 51.79 | 100.00 |
| Meghalaya | 13.80 | 32.53 | 417.38 | | 4.15 | 467.86 | 5.06 | 100.00 |
| Mizoram | | 41.47 | 97.94 | | 8.01 | 147.42 | 20.72 | 93.98 |
| Nagaland | | 31.67 | 66.33 | | 3.04 | 101.04 | 32.89 | 100.00 |
| Odisha | 59.22 | 115.63 | 2163.22 | | 452.67 | 2790.74 | 93.94 | 5.09 |
| Pondicherry | | | | | 35.53 | 35.53 | 99.49 | 97.74 |
| Punjab | 498.94 | 176.10 | **3818.28** | | 1127.07 | 5620.39 | 93.28 | 21.19 |
| Rajasthan | 125.08 | 23.85 | 1941.93 | **4576.82** | **15,283.66** | **21,951.34** | 96.87 | 5.64 |
| Sikkim | | 55.11 | 633.00 | | 4.68 | 692.79 | 58.97 | 100.00 |
| Tamil Nadu | **1042.70** | 123.05 | 2178.20 | **9873.92** | **6233.36** | **19,451.23** | 99.04 | 5.97 |
| Telangana | 219.74 | 90.87 | 2479.93 | 128.10 | **4637.39** | 7556.03 | 99.81 | 5.79 |
| Tripura | | 16.01 | 68.49 | | 16.26 | 100.76 | 57.87 | 46.87 |
| Uttar Pradesh | **2192.89** | 49.10 | **3424.03** | | 2264.78 | 7930.80 | 94.06 | 12.15 |
| Uttarakhand | 139.44 | **218.82** | 2095.89 | | 575.45 | 3029.60 | 97.51 | 46.82 |
| West Bengal | 323.70 | 98.50 | 1396.00 | | 176.03 | 1994.23 | 92.62 | 32.53 |
| All-India total | **10,700.84** | **4899.50** | **45,687.52** | **41,661.78** | **60,768.92** | **163,718.56** | **96.61** | **12.80** |

*Note*: Blank spaces indicate no installed capacity. Bold values indicate installed capacity for a given state is in the top five. Large hydro data are from Central Electricity Authority, all other data are from the Ministry of New and Renewable Energy. CEA data do not distinguish between Jammu & Kashmir and Ladakh, and so the total large hydro capacity for the two regions is entered only under Jammu & Kashmir. MNRE data are available from https://mnre.gov.in/img/documents/uploads/file_s-1665464058867.pdf. See Section 2.2.2 for information on CEA data.